THE JOURNAL OF PHYSICAL CHEMISTRY B
A JOURNAL OF THE AMERICAN CHEMICAL SOCIETY

pubs.acs.org/JPCB

Perspective

Shape-Changing Bottlebrush Polymers

Bin Zhao*

Cite This: *J. Phys. Chem. B* 2021, 125, 6373–6389

Read Online

ACCESS | Metrics & More | Article Recommendations

ABSTRACT: Bottlebrush polymers (BBPs), composed of relatively short polymeric side chains densely grafted on a polymer backbone, exhibit many unique characteristics and hold promise for a variety of applications. This Perspective focuses on environmentally induced shape-changing behavior of BBPs at interface and in solution, particularly worm/star−globule shape transitions. While BBPs with a single type of homopolymer or random copolymer side chains have been shown to undergo pronounced worm-to-globule shape changes in response to external stimuli, the collapsed brushes are unstable and prone to aggregation. By introducing a second, solvophilic polymer into the side chains, either as a distinct type of side chain or as the outer block of block copolymer side chains, the collapsed brushes not only are stabilized but also create unimolecular micellar nanostructures, which can be used for, e.g., encapsulation and delivery of substances. The current challenges in the design, synthesis, and characterization of stimuli-responsive shape-changing BBPs are discussed.

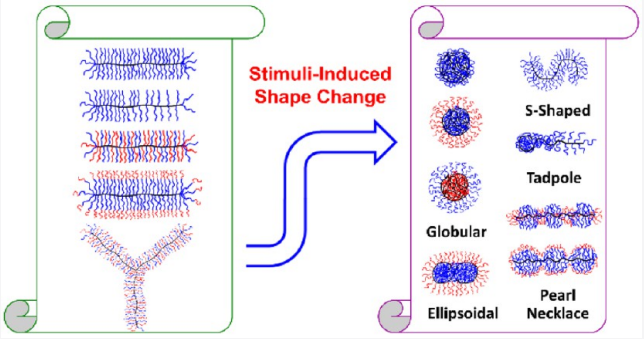

INTRODUCTION

Bottlebrush polymers (BBPs), also called molecular (bottle)-brushes, are a special class of graft copolymers in which relatively short polymeric side chains are densely grafted via a covalent bond on a polymer backbone.[1−5] These complex macromolecules have attracted tremendous interest in past decades; significant effort has been made to develop synthetic methods, characterize their molecular structures and conformations, understand their behavior and properties in bulk and solution states, and explore their potential applications. Experimental, theoretical, and simulation studies have revealed many intriguing characteristics and behavior of BBPs, including the giant molecular dimension and anisotropic shape,[1−5] high density of functional groups,[1] large and tunable persistence length,[2,3] stimuli-induced pronounced shape change,[2−4] extremely high backbone entanglement molecular weight,[6] and unusual crystal habit,[7] all of which originate from the brushes' dense grafting nature. Promising applications of BBPs have been demonstrated in diverse areas, ranging from photonic crystals[8] to surface coatings for lubrication,[9] supersoft elastomers,[6] drug delivery systems,[10] and template synthesis of nanomaterials.[11]

The molecular structure of BBPs in the most basic form (i.e., a linear backbone with single-component homopolymer side chains, Figure 1a) can be defined by three molecular parameters: the degree of polymerization (DP) of the backbone (N_{bb}), the DP of side chains (N_{sc}), and the average distance between two neighboring side chains (d_{sc}) or more commonly the grafting density of side chains (σ_{sc}). The latter is commonly expressed as the percentage of backbone monomer units that carry a side chain. The σ_{sc} is sufficiently high that the distance between the tethering points of neighboring side chains on the backbone is smaller than the side chains' unperturbed size. The steric repulsive interactions between the densely grafted side chains cause the backbone and side chains of BBPs to take on stretched conformations, similar to the surface polymer brushes on solid substrates;[12] at a sufficiently large ratio of N_{BB} to N_{SC}, brush molecules exhibit a persistent cylindrical shape in good solvents, even if the backbone and side chains are both flexible polymers.[1−3] The anisotropic molecular shape of BBPs is in stark contrast to linear flexible polymer chains in good solvents, which are random coils with a spherical shape on average over time or ensemble (Figure 1b).[13] The equilibrium length of brush molecules in a good solvent is determined by the interplay of the extension force from repulsive interactions between side chains and the entropic retraction force from backbone stretching. The persistence length (L_P) or Kuhn length of BBPs can be readily tuned by varying N_{SC} and σ_{SC} as well as the type of backbone and side chain polymers.[3,14] In general, L_P increases with increasing N_{SC} and σ_{SC}; for example, for BBPs with poly(*n*-butyl acrylate)

Received: March 1, 2021
Revised: May 4, 2021
Published: May 27, 2021

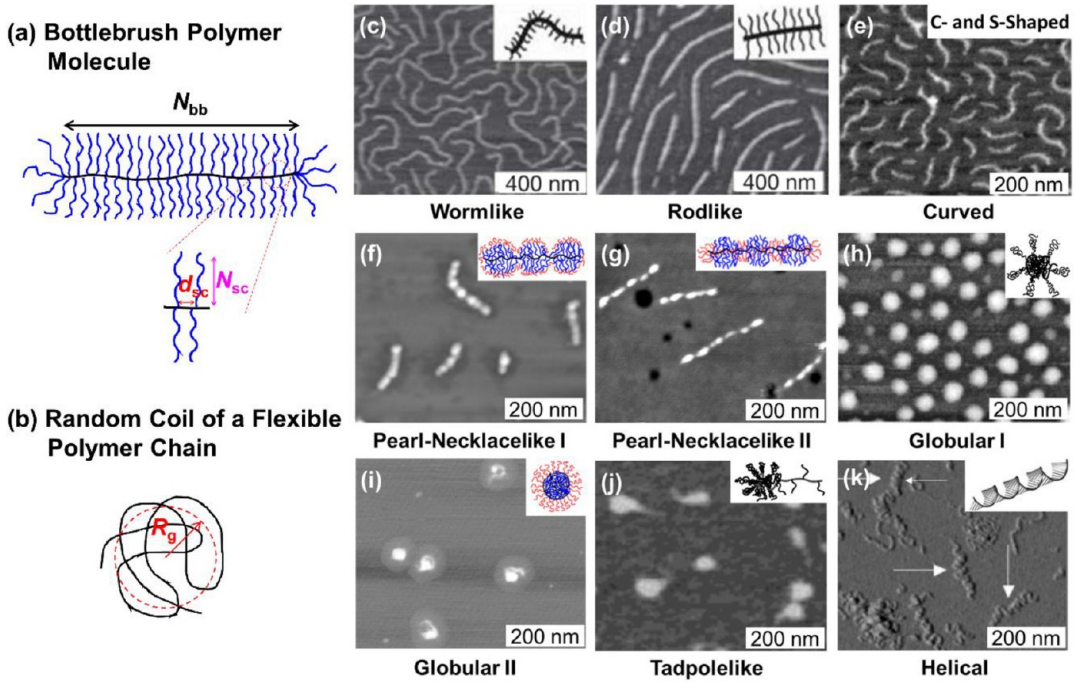

Figure 1. (a, b) Schematics of a bottlebrush molecule with single-component homopolymer side chains (a) and a random coil of a linear flexible polymer chain (b). N_{bb}: degree of polymerization of the backbone. N_{SC}: degree of polymerization of side chains. d_{sc}: distance between neighboring side chains. R_g: radius of gyration. (c–k) Various shapes of linear BBPs observed experimentally: wormlike (c), rodlike (d), C- and S-shaped (e), pearl-necklace (f, g), globular (h, i), tadpole (j), and helical (k). (c, d) Reprinted with permission from ref 14. Copyright 2006 Springer Nature. (e–j) Reprinted and adapted with permission from refs 17, 11, and 18–21, respectively. Copyright 2004, 2004, 2020, 2001, 2018, and 2004 American Chemical Society, respectively. (k) Reprinted and adapted with permission from ref 22. Copyright 2008 Wiley-VCH.

(P*n*BA) side chains on mica, atomic force microscopy (AFM) studies show that the L_p strongly depends on N_{SC} in a scaling relationship of $L_p \propto DP_{SC}^{2.7}$.[14]

One intriguing characteristic of BBPs with a flexible backbone is that the backbone is locally flexible on the length scale of monomer units, as reflected in the fast decay of the bond angle correlation at this length scale from simulation studies,[15,16] while displaying a large directional persistence at greater length scales. In other words, such a BBP backbone can coil locally but maintain extended conformations due to the densely grafted side chains. This characteristic renders it possible for BBPs to exhibit distinct shapes under different conditions. If different polymers are introduced into the side chains, a variety of multicomponent BBPs are possible,[3] such as heterografted BBPs with distinct side chains distributed along the backbone in a uniform or a gradient fashion and homografted BBPs with block copolymer side chains, which further enrich the conformational behavior of BBPs. Through judicious control of environmental conditions, many different shapes have been experimentally observed for linear single- and multicomponent BBPs. These include wormlike (Figure 1c),[14] rodlike (Figure 1d),[14] C- and S-shaped (Figure 1e),[17] pearl-necklace (Figure 1f,g),[11,18] spherical (Figure 1h and i),[19,20] tadpole (Figure 1j),[21] and helical conformations (Figure 1k).[22] BBPs can be induced to convert from one shape to another by external stimuli.[17−22] For example, when P*n*BA BBP molecules on the water surface are laterally compressed in a Langmuir–Blodgett (LB) trough, pronounced rod-to-sphere shape transitions are observed.[19] Moreover, for multicomponent BBPs, the worm-to-globule shape transitions are accompanied by reversible formation of unimolecular core–shell micellar nano-objects,[20,23] which could be used, for example, as drug carriers.[23]

This Perspective focuses on the stimuli-responsive shape-changing behavior of BBPs, particularly worm/star–globule shape transitions. After an introduction to the synthesis of BBPs, I will first discuss the shape changes of homografted BPPs that comprise a single type of homopolymer or random copolymer side chains at the interface and in solution triggered by various environmental stimuli. One main issue with such BBPs is the high propensity of collapsed brushes to aggregate. To stabilize the collapsed globular brushes, a second, solvophilic polymer can be introduced into the side chains,[20,23] either as a second type of side chains or as the outer block of block copolymer side chains, which will be the focus of the next section—stimuli-induced shape transitions of multicomponent BBPs. Last, the current challenges in the design, synthesis, characterization, and applications of stimuli-responsive shape-changing BBPs will be highlighted.

SYNTHESIS OF BOTTLEBRUSH POLYMERS

Considering the architecture and the chemical composition, there are numerous possible BBPs that can be envisioned.[2,3] In terms of topology, the backbone could be linear, star-shaped, cyclic, or regularly or irregularly branched, and the polymer for the backbone could be flexible or stiff, with the ability to carry a side chain every two or five backbone carbon atoms at the highest grafting density. The side chains could be a homopolymer, a random copolymer, a block copolymer, or a mixture of two or more different polymers. If side chains contain different polymers, they could be distributed along the backbone in a uniform or gradient fashion. Despite numerous possible architectures and compositions, BBPs are synthesized by one or a combination of three basic methods: grafting from, grafting to, and grafting through (Scheme 1).[1−5]

https://doi.org/10.1021/acs.jpcb.1c01819
J. Phys. Chem. B 2021, 125, 6373−6389

Scheme 1. Synthesis of Linear Bottlebrush Polymers by Grafting from (a and d), Grafting to (b and e), and Grafting through (c and f) with an Example for Each Method

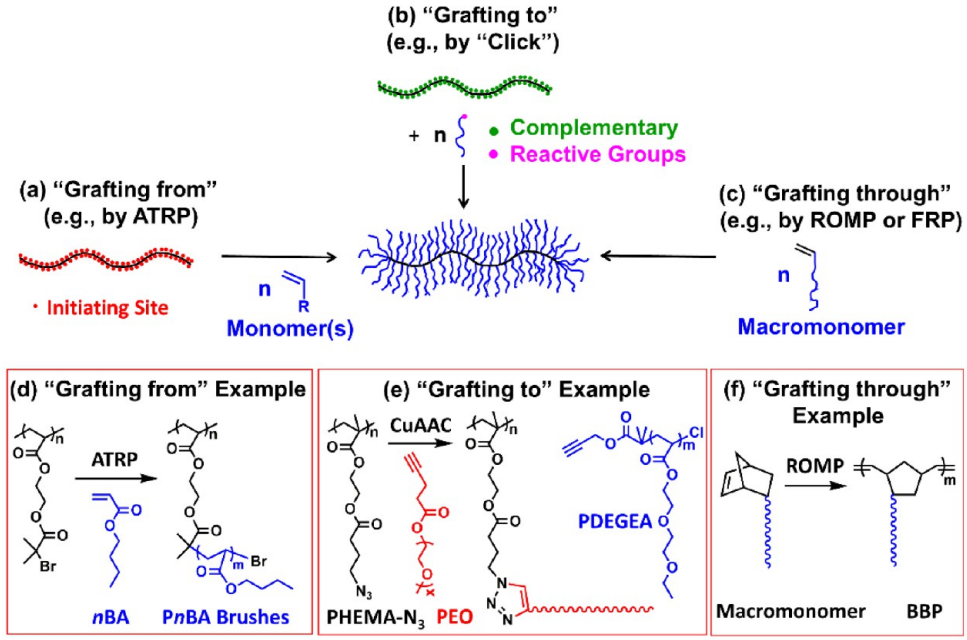

"Grafting from" is widely employed for the synthesis of BBPs (Scheme 1a). In this approach, a macroinitiator is prepared first,[1−3] either directly or indirectly via postpolymerization modifications. The use of a "living" polymerization technique such as atom transfer radical polymerization (ATRP) or ring-opening metathesis polymerization (ROMP) for the preparation of macroinitiators or their precursors is highly desired as it can produce narrow dispersity polymers, which will lead to more uniform bottlebrush molecules. Subsequently, side chains are grown from the pendant initiating sites of the macroinitiator in a controlled manner, e.g., by ATRP,[14,19,24,25] ring-opening polymerization,[24] or reversible addition−fragmentation chain transfer (RAFT) polymerization.[25] For ATRP, the polymerization is typically stopped at low monomer conversions to minimize the side reactions of propagating radicals in close proximity and to avoid interbrush cross-linking. As an example, the synthesis of P*n*BA BBPs is shown in Scheme 1d.[19] In general, "grafting from" produces high density BBPs,[14,19] although low σ_{SC} values (e.g., 50%) have also been reported.[26] It is suited for the synthesis of homografted BBPs with the same type of side chains such as homopolymer or block copolymer side chains. For example, Zhang et al. prepared core−shell BBPs with diblock copolymer side chains and used them for the templated synthesis of nanoparticles in the core of the brushes.[1,11] For heterografted BBPs containing different types of side chains, this method is more difficult to apply, as it often requires different polymerization methods for different types of side chains.[24,25]

In the "grafting to" approach (Scheme 1b), an end-functionalized polymer or a mixture of end-functionalized polymers reacts with a backbone polymer that bears complementary pendant reactive groups.[27] This method is modular; the backbone and side chain polymers are synthesized separately, allowing for thorough characterization prior to assembling them into BBPs. Moreover, the molar ratio of the pendant groups on the backbone and the end-functionalized side chains as well as the molar ratio(s) of different side chain polymers can be readily tuned in the feed, enabling the synthesis of a large number of BBPs from the same backbone and side chain polymers with different grafting densities and compositions. Historically, "grafting to" was not a very viable method for the synthesis of high grafting density BBPs. However, with the advent of highly efficient click reactions such as copper(I)-catalyzed azide−alkyne cycloaddition (CuAAC), high density BBPs can be routinely synthesized.[7,18,20,23,27,28] Scheme 1e shows the synthesis of poly(ethylene oxide) (PEO) BBPs via CuAAC. A drawback of "grafting to" is the need to remove unreacted side chains from the formed BBP, which can be difficult. However, repeated fractionation or centrifugal filtration can completely remove the remaining unreacted side chains from the brushes.[7,18]

In the "grafting through" approach (Scheme 1c), a macromonomer (i.e., a polymer having a polymerizable group at one end) or a mixture of macromonomers is polymerized directly to produce a BBP. The advantage of this method is that the BBP has a perfect grafting density of 100%. The "grafting through" synthesis of BBPs in earlier days was mainly accomplished by conventional free radical polymerization (FRP) of methacrylate- or styrenic-end-functionalized macromonomers, which often proceeded to only low conversions likely due to the high steric hindrance and the low concentration of the polymerizable groups.[29] Using highly active Grubbs catalysts, well-defined homo- and heterografted BBPs with a high backbone DP can be readily prepared by ROMP (Scheme 1f).[30−32] It should be noted here, however, that each repeat unit in polynorbornene BBPs contains five carbon atoms, in contrast to two carbon atoms in one repeat unit of BBPs with a vinyl polymer backbone.

More complex BBPs can be synthesized by a combination of the three basic methods.[28,33] For example, Ishizu et al. prepared diblock BBPs by combining "grafting through" and "grafting from" approaches.[33] They first polymerized 2 kDa oligo(ethylene glycol) methyl ether methacrylate and then 2-hydroxyethyl methacrylate to produce brush-coil diblock copolymers. After the conversion of the pendant hydroxyl groups on the second block to ATRP initiating moieties, side

https://doi.org/10.1021/acs.jpcb.1c01819
J. Phys. Chem. B 2021, 125, 6373−6389

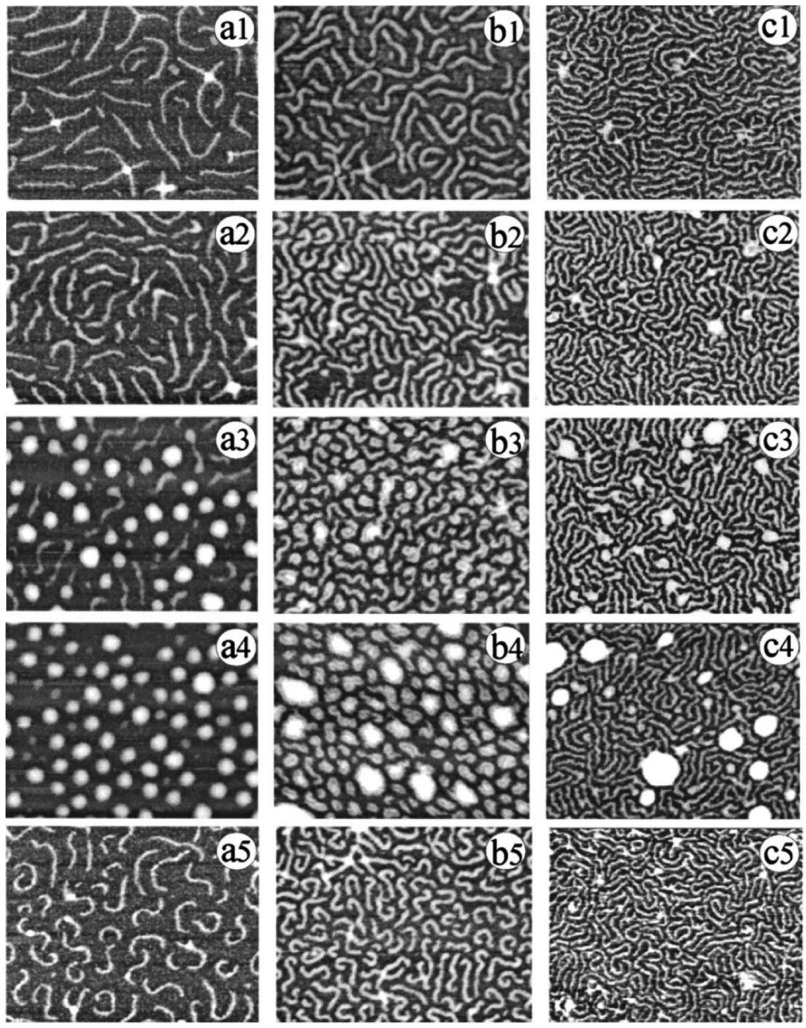

Figure 2. AFM micrographs ($600 \times 400\ \mu m^2$) of the monolayers of P*n*BA BBPs (BBP-A, a1−a5; BBP-B, b1−b5; BBP-C, c1−c5) transferred on mica at different degrees of compression: (a1, b1, c1) A_{nBA} = 31 Å^2; (a2, b2, c2) 21 Å^2; (a3, b3, c3) 17 Å^2; (a4, b4, c4) 13 Å^2; (a5, b5, c5) 31 Å^2 (after expansion). Reprinted with permission from ref 19. Copyright 2001 American Chemical Society.

chains were grown from the backbone, yielding diblock BBPs. Although different or the same methods can be used sequentially, repeatedly, or simultaneously to synthesized multicomponent BBPs,[24,25,28,33] the characterization of the brushes' molecular structures becomes increasingly challenging. Thus far, shape-changing BBPs that are reported in the literature contain no more than two distinct polymers in the side chains, either in the form of homografted diblock copolymer side chains or heterografted side chains, which can be made by "grafting from" or "grafting to". More complex stimuli-responsive shape-changing BBPs will require more careful consideration of synthetic methods.

■ ENVIRONMENTALLY INDUCED SHAPE TRANSITIONS OF BBPS WITH A SINGLE TYPE OF HOMOPOLYMER OR RANDOM COPOLYMER SIDE CHAINS

Environmentally induced shape changes of BBPs that consist of a single type of homopolymer or random copolymer side chains have been demonstrated at air−water interfaces, on solid substrates, and in solutions by various means, including mechanical compression,[19] exposure to different vapors,[34,35] temperature changes,[36] and pH variations.[37] AFM, which can be performed on brush molecules in the dry state and adsorbed on a substrate in a solution, is the predominant characterization technique used to visualize the conformational transitions of BBPs.

Desorption-Induced Shape Transitions of BBPs with a Single Type of Homopolymer Side Chains at the Air−Water Interface. The very first remarkable rod−globule shape transition of single BBP molecules was reported by Sheiko et al.[19] Three linear P*n*BA BBPs were synthesized by ATRP "grafting from" (Scheme 1d): BBP-A (N_{BB} = 641; N_{SC} = 48), BBP-B (N_{BB} = 453; N_{SC} = 20), and BBP-C (N_{BB} = 490; N_{SC} = 15). These brushes were deposited onto the water surface in an LB trough, spreading out to maximize the contacts of polar ester groups with water, and then laterally compressed to different degrees, characterized by the occupied surface area per P*n*BA monomer unit (A_{nBA}). The brush monolayers were transferred to mica for visualization by AFM. Prior to compression, the brushes were either rodlike (BBP-A, Figure 2a1) or wormlike (BBP-B and C, Figure 2b1,c1). With the increase of the compression, BBP-A and -B underwent a striking shape transition to globular (Figure 2a2−a4,b2−b4). While BBP-A in Figure 2a4 was nearly spherical, the collapsed BBP-B was more ellipsoidal with the backbone visible (Figure 2b4). In

https://doi.org/10.1021/acs.jpcb.1c01819
J. Phys. Chem. B 2021, 125, 6373−6389

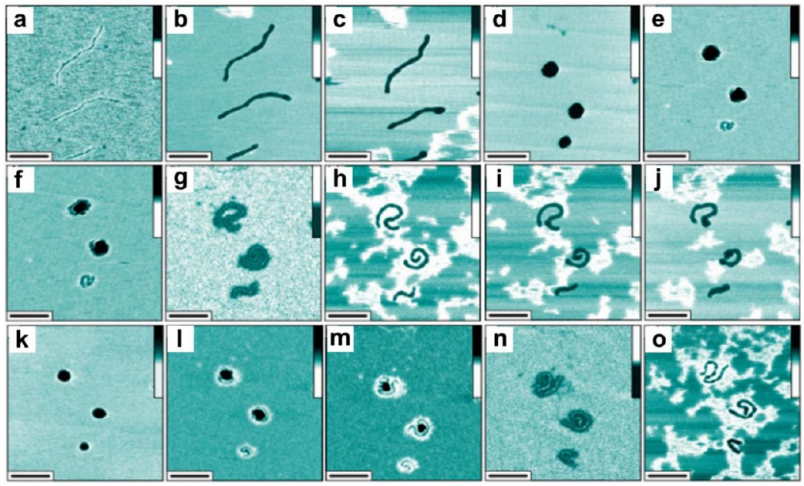

Figure 3. Sequence of AFM images showing the collapse and expansion for P*n*BA bottlebrushes with an N_{BB} of 3700 and an N_{SC} of 30 on mica in vapors saturated with humidified ethanol (80 vol %) and water: (a) initial image of the deposited molecules; (b, c, h, i, j, o) images obtained 9 min (o), 18 min (b, h), 27 min (c, i), and 36 min (j) after the injection of humidified ethanol to the environmental chamber; (a, d, g, k, n) images taken in dry N_2; (e, f, l, m) images recorded 27 min (e), 36 min (f, l), and 54 min (m) after the injection of water. Scale bar: 250 nm. Height scale: 10 nm. Reprinted and adapted with permission from ref 35. Copyright 2004 Wiley.

contrast, BBP-C with an N_{SC} of 15 remained in the wormlike state. These observations revealed the importance of N_{SC} in the shape transition of BBPs; the longer the side chains were, the more pronounced the shape change was, and there existed a critical value for N_{SC}, below which no shape change would occur. Interestingly, Figure 2a3 shows the coexistence of wormlike and globular brushes, indicating that the shape transition was a "pseudo"-first-order phase transition. Upon expansion, the globular BBPs were unfolded to wormlike (Figure 2a5,b5), many of which were C- or S-shaped (also see Figure 1e). Theoretical analysis showed that an uneven distribution of P*n*BA side chains on the two sides of the backbone increased the entropy of the absorbed BBPs.[17] The observed shape change was triggered by the surface compression-induced desorption of P*n*BA side chains from the water surface. At higher compression, a portion of side chains desorbed from the water surface, and the minimization of the surface area of desorbed side chains caused the contraction of the brushes and the coiling of the backbone, resulting in a globular shape. On the basis of the balance of the interfacial energy, which decreases upon energetically favorable adsorption of P*n*BA on water, and the elastic energy, which increases upon adsorption due to the entropically unfavorable extension of the backbone and side chains,[19] scaling analysis of P*n*BA BBPs on water showed a "pseudo"-first-order rod−globule transition upon varying the spreading coefficient or lateral compression and a critical N_{SC} value, consistent with experimental results.

Besides linear P*n*BA BBPs, four-armed star BBPs with P*n*BA side chains were also shown to exhibit reversible shape changes from starlike to disklike on the water surface upon lateral compression.[38] Interestingly, the collapsed disklike brushes, with a height much smaller than the width, were found to be more ordered compared with collapsed linear BBPs; domains with nearly perfectly hexagonal packing were easily seen from the AFM images. This could be attributed to the lower dispersity ($Đ_{star}$) of star BBPs compared with that of the individual arms because $Đ_{star} = (Đ_{arm}/f) + (f - 1)/f$, where f is the number of arms in the star polymer.[38]

As shown in Figure 2, N_{SC} must be above a threshold value for BBPs to exhibit a worm−globule shape transition.[19] Another molecular parameter that also plays an important role in the shape transition is σ_{SC}. Theoretical analysis showed that higher grafting density BBPs undergo shape transitions more readily than lower density brushes.[39] This was proven by Lord et al. using linear gradient P*n*BA BBPs,[21] in which the σ_{SC} changed gradually along the backbone from one end to another. Such gradient BBPs were synthesized by taking advantage of different reactivity ratios of methyl methacrylate and 2-(trimethylsilyloxy)ethyl acrylate in the copolymerization, followed by the installation of ATRP initiating groups and the growth of P*n*BA side chains. After the brushes were deposited on water and compressed, the densely grafted end of the brushes collapsed into a globular head while the loosely grafted end remained extended as a tail, resulting in a tadpole shape, which was better seen in the linear P*n*BA matrix (Figure 1j). It is striking to see different parts of one brush molecule exhibit different conformations under the same condition, indicating that there exists a critical σ_{SC} below which there would be no shape transition even at high compression. This was confirmed using two homogeneous P*n*BA BBPs with σ_{SC} values of 23% and 65%.[21] While the BBP with the σ_{SC} of 65% readily underwent a worm-to-globule transition when compressed, no shape change was observed for the BBP with the σ_{SC} of 23%.

The shape of P*n*BA BBPs at the water−air interface depends on the fraction of P*n*BA side chains adsorbed on the water surface and can be induced to change through lateral compression as shown above.[19,21,38] Alternatively, one can lower the surface free energy (γ) of the aqueous solution to trigger the shape change of P*n*BA BBPs at the water−air interface by weakening the interactions between P*n*BA and water, as shown by Sun et al. through the addition of methanol into water.[40] Water and methanol have rather different γ values at 25 °C, 72 and 23 mM/m, respectively, which allow for tuning the γ of the water−methanol solution by varying their ratio. A P*n*BA BBP with an N_{BB} of 567 and an N_{SC} of 35 was spread on the surfaces of a series of water−methanol mixtures with different methanol contents, transferred onto mica, and imaged by AFM. The average brush length was found to decrease with increasing methanol proportion. At a methanol percentage of 21% (γ = 47.2 mN/m), most of the brushes changed to a

https://doi.org/10.1021/acs.jpcb.1c01819
J. Phys. Chem. B 2021, 125, 6373−6389

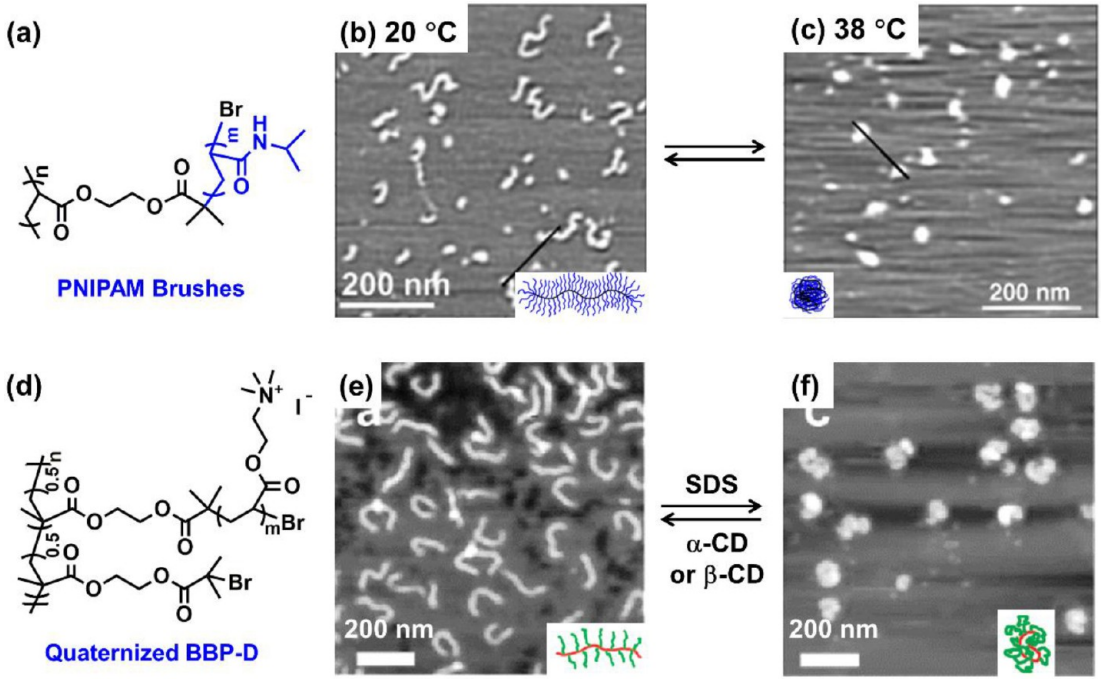

Figure 4. Shape-changing behavior of stimuli-responsive BBPs with a single type of homopolymer side chains in aqueous solutions. (a) Molecular structure of a PNIPAM BBP and AFM height images of the PNIPAM BBP in water at 20 °C (b) and 38 °C (c). Reprinted and adapted with permission from ref 36. Copyright 2004 Wiley-VCH. (d) Molecular structure of the CH_3I-quaternized PDMAEMA BBP-D and AFM height images of the resultant polyelectrolyte BBP in the wormlike state (e) and globular state (f). Reprinted and adapted with permission from ref 56. Copyright 2009 American Chemical Society.

globular shape, while a small number of molecules remained wormlike. Further increasing the methanol fraction to 22% (γ = 46.7 mM/m) caused all brushes to collapse into a globular shape; some large aggregates appeared, likely due to the lack of stabilization of globular brushes. These experiments unequivocally demonstrated that BBPs can spontaneously change their shapes according to environmental conditions.

Solvent Vapor-Induced Shape Transitions of BBPs with a Single Type of Homopolymer Side Chains on Solid Substrate. P*n*BA BBPs have also been shown to undergo shape transitions on solid substrates upon exposure to different solvent vapors.[34,35,41] Using environmentally controlled AFM, Gallyamov et al. visualized the worm−globule shape changes of P*n*BA BBPs on solid substrates in situ in real time by introducing different solvent vapors into the sample chamber.[34,35] The wormlike P*n*BA brushes spin-cast on mica were observed to swell but did not contract when ethanol was introduced into the chamber. Intriguingly, after a small amount of water was added into the chamber, the worm-to-globule transition began, where water appeared to act as a lubricant by increasing the brushes' mobility on the surface. The shape change started with forming small nodules preferentially at the brush ends, which increased in size and gradually moved toward the center of the molecule until the two nodules merged into an individual globule. After drying of the chamber with N_2 and addition of water, the globular brushes expanded and untwined. Figure 3 shows the worm−globule shape transitions of P*n*BA brushes on mica;[35] after the first cycle, the brush molecules displayed a distinct curvature, similar to those in Figures 1e and 2a5 due to the gain in entropy from the bending of the backbone.[17,19]

The composition of the water−ethanol vapor was critical for the brushes' shape transition.[34,35] The change of the P*n*BA BBP from a wormlike to a globular conformation was observed after the addition of a water−ethanol mixture with 30 vol % or more of ethanol, but no collapse occurred when the ethanol content was 20 vol % or less. The γ of pure ethanol is 22 mN/m, much lower than that of water. Both water and ethanol adsorbed onto the mica surface and formed an adlayer, which modulated the interactions of the P*n*BA brushes with the substrate. The brushes spread at higher water contents (i.e., high γ) and shrank at higher ethanol contents (i.e., lower γ). At the critical composition of the water−ethanol mixture where no spreading and shrinking occurred, the γ of the mixture was similar to that of P*n*BA. Thus, the observed shape transition of the BBP is similar in principle to that on the water−methanol surface induced by varying the γ of the liquid mixture.

Besides ethanol, many amphiphilic organic liquids with a low surface tension (γ < 25 mN/N), such as methanol, isopropanol, diethyl ether, and ethyl acetate, can be used to trigger the collapse of P*n*BA BBPs on mica.[41] On the other hand, higher surface tension liquids, such as ethylene glycol, dimethyl sulfoxide, and *N*,*N*-dimethylformamide, were found to induce the globule-to-worm shape transition of P*n*BA brushes. Similar to ethanol, low surface tension amphiphilic liquids can be uptaken by the brushes on mica but cannot initiate the transition. A small amount of water is necessary to start the collapse. The shape transitions of P*n*BA BBPs have also been observed on silicon and $SrTiO_3$ substrates upon exposure to different solvent vapors.[42] Interestingly, unlike on mica, ethanol can induce the worm-to-globule transition on silicon substrates without water. An exciting attempt has been made to use vapor-triggered shape changing of P*n*BA BBPs on solid substrates to develop molecular walkers with directed motions.[42]

Stimuli-Induced Shape Transitions of BBPs with a Single Type of Homopolymer or Random Copolymer Side Chains in Solution. Stimuli-responsive polymers exhibit

https://doi.org/10.1021/acs.jpcb.1c01819
J. Phys. Chem. B 2021, 125, 6373−6389

relatively large physical or chemical changes in response to environmental stimuli, often accompanied by dramatic conformational and solubility changes in solvents.[43] Numerous polymers that can respond to various external stimuli, such as pH,[44] temperature,[45−47] and light,[48] have been reported. When these polymers are employed as side chains, the physical properties of the BBPs in solution can be readily controlled through external stimuli.[20,26,36,37,49−66] Compared with mechanical compression or treatment with solvent vapors for BBPs at interfaces, it is much more convenient to apply common stimuli to the BBPs in solution. Moreover, such stimuli-responsive BBPs are more relevant to potential applications, e.g., encapsulation and release of substances.

BBPs with a single type of responsive homopolymer or random copolymer side chains have been shown to exhibit size or solubility changes in solutions in response to external stimuli, such as temperature, pH, ionic strength, or solvent variations, or the addition of surfactants, specific ions, or polyelectrolyte, although explicit shape transitions of these brushes are not always clearly discussed. The first example of dramatic worm−globule shape transitions of BBPs in solution was reported by Li et al.[36] Using an ATRP "grafting from" method, they synthesized a BBP comprising poly(*N*-isopropylacrylamide) (PNIPAM) side chains (Figure 4a). PNIPAM is a thermoresponsive polymer with a lower critical solution temperature (LCST) of 32 °C in water. Upon heating, the R_g of the BBP in water first showed a gradual decrease from 61 nm at 20 °C to ∼40 nm at 31 °C, followed by a sharp decrease to 25 nm within only 0.5 °C. AFM revealed wormlike molecules at 20 °C both in the dry state and in water (Figure 4b) with essentially the same lengths. Upon heating across the LCST, the BBP transformed into globular and ellipsoidal nano-objects as seen by AFM in water (Figure 4c). However, the collapsed brushes were unstable above 38 °C; aggregation and eventually precipitation occurred.

Poly(*N*,*N*-dimethylaminoethyl methacrylate) (PDMAEMA) is a special thermosensitive polymer, whose LCST behavior in water depends on solution pH and is only observed at higher pH values. Lee et al. synthesized a PDMAEMA BBP and observed that at a 0.1 wt % concentration the brushes underwent shrinking upon heating, with the hydrodynamic size (D_h) decreasing from 61 nm at 20 °C to 34 nm at 55 °C.[49] However, at a higher concentration, intermolecular aggregation occurred upon heating. Similar concentration-dependent thermoresponsive behavior was also reported by Pietrasik et al., who synthesized thermoresponsive BBPs composed of a statistical copolymer of either DMAEMA and methyl methacrylate or *N*,*N*-dimethylacrylamide and *n*-butyl acrylate as side chains.[50] Incorporation of a small amount of different stimuli-responsive functional groups into thermosensitive polymers can produce multiresponsive polymers, which can be used to make multiresponsive BBPs with a single type of random copolymer side chains. Lee et al. copolymerized an azobenzene-containing monomer into PDMAEMA and demonstrated the tuning of the thermoresponsive behavior of BBPs in water by UV irradiation.[49] Yamamoto et al. synthesized dually responsive BBPs consisting of statistical copolymers of methoxydi(ethylene glycol)methacrylate and either methacrylic acid or DMAEMA or both. The LCST transitions of these brush polymers were shown to depend on solution pH.[51] However, no studies on shape transitions were reported for these BBPs with random copolymer side chains.[49,51] Henn et al. synthesized BBPs homografted with light-responsive and thermoresponsive random copolymer side chains and demonstrated by both AFM and dynamic light scattering (DLS) multiple cycles of worm−globule shape transitions through judicious control of heating and UV irradiation.[52]

pH-responsive polymers are another class of widely studied stimuli-sensitive polymers, which usually contain pendant weak acid or base groups.[44] Lee et al. synthesized poly(acrylic acid) (PAA) BBPs by ATRP grafting from and studied their conformations by AFM after spin-casting of the brushes on mica from aqueous solutions of different pH values.[37] For the fully grafted PAA BBP synthesized from the macroinitiator derived from a homopolymer precursor of 2-(trimethylsilyloxy)-ethyl methacrylate (HEMA-TMS), the brushes exhibited similar cylindrical conformations in the pH range 2−9, likely due to the strong adsorption on mica. Interestingly, for loosely grafted PAA BBPs made from the macroinitiators synthesized from the copolymers of methyl methacrylate and HEMA-TMS with the HEMA-TMS content ≤20 mol %, the brushes exhibited a gradual transition from a compact globular to a more extended wormlike conformation with the increase of pH from ∼4 to ∼9. The transition was caused by the repulsive interactions between the side chains at higher pH. However, it should be noted here that the brushes aggregated at lower pH values as observed from DLS even at a concentration as low as 0.3 mg/g. Xu et al. synthesized two PDMAEMA BBPs from the same macroinitiator by ATRP "grafting from".[26] The initiating efficiencies for both were found to be only ∼50%, and there were ∼750 side chains with N_{SC} values of 65 and 82 for the two BBPs. DLS measurements of the BBP with an N_{SC} of 82 (BBP-D) was conducted at 0.2 mg/mL to avoid intermolecular aggregation; the D_h was found to increase from ∼33 to ∼43 nm when the pH decreased from 10 to 2. Cryo-transmission electron microscopy (cryo-TEM) of BBP-D in 0.01 mg/mL solutions showed that the brushes adopted a stretched morphology at pH = 2.0 and appeared to be wormlike at pH = 7.0. The brushes strongly contracted at pH = 10 but were still wormlike because PDMAEMA is soluble in both acidic and basic water. Unlike PDMAEMA, poly(*N*,*N*-diethylaminoethyl methacrylate) (PDEAEMA) is a pH-responsive polymer with a pK_a of 7.4 that exhibits a soluble-to-insoluble transition upon increasing the pH from below to above the pK_a.[44,67] Kent et al. showed that a BBP homografted with PDEAEMA side chains precipitated out immediately when the aqueous solution pH was increased to >7.3 even at a concentration as low as 0.2 mg/g.[53]

Polyelectrolyte BBPs with permanently charged side chains are an intriguing class of responsive BBPs as they exhibit rich conformational behavior in response to the variations of ionic strength and the addition of specific ions, small molecule surfactants, and linear polyelectrolytes. One of the most prominent characteristics of polyelectrolyte BBPs is the confinement of counterions within the brushes in pure water, resulting in a very high osmotic pressure and forcing the brushes to exhibit extended conformations.[54,68] Any external factors that can change the osmotic pressure within the brushes could cause a shape change. Xu et al. made a quaternary ammonium-based polyelectrolyte BBP by quaternizing the aforementioned PDMAEMA BBP with an N_{SC} of 82 (BBP-D) using iodomethane (Figure 4d).[26] The wormlike shape was confirmed by AFM of the brushes on mica and also cryo-TEM of the brushes in the vitrified solution. This cationic BBP exhibited salt-responsive behavior in aqueous solution; the D_h of the brushes decreased from 87 nm in pure water to ∼72 and ∼70 nm at 0.5 and 1.0 M NaBr, respectively. AFM showed that the brushes spin-cast on mica from 0.5 M NaBr were in a collapsed

https://doi.org/10.1021/acs.jpcb.1c01819
J. Phys. Chem. B 2021, 125, 6373−6389

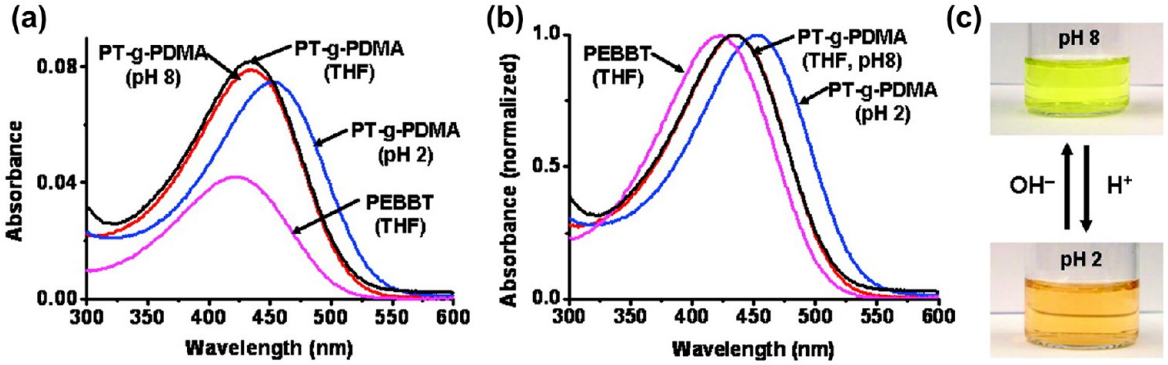

Figure 5. (a) Absorption spectra and (b) normalized absorption spectra of 2,5-poly(3-(1-ethyl-2(2-bromoisobutyrate))thiophene) (PEBBT macroinitiator) in THF and 2,5-poly(3-[1-ethyl-2(2-(poly(*N*,*N*-dimethylaminoethyl methacrylate))]thiophene) (PT-*g*-PDMA) (0.1 mg/mL) in THF, in water at pH 8 and at pH 2. (c) Digital photographs of the PT-*g*-PDMA brushes in water at pH 8 and pH 2. Reprinted and adapted with permission from ref 71. Copyright 2008 American Chemical Society.

ellipsoidal or globular shape.[26] Remarkably, they found that with the addition of divalent $[Ni(CN)_4]^{2-}$ or trivalent $[Co(CN)_6]^{3-}$ anions at a BBP concentration of 0.02 mg/mL the brushes took on a helical conformation with a helical pitch of 25 nm in the intermediate state when the brushes changed from a cylindrical to a globular state.[55] No helical structure was observed upon the addition of monovalent ions. The helix formation was suggested to be a result of an overlap of the excluded volume from successive turns arising from the interactions with multivalent anions, which increased the entropy of the system.[55]

Besides the ionic strength and the ion valency, the morphology of polyelectrolyte BBPs in aqueous solutions can also be manipulated by the addition of surfactants. Xu et al. reported that the quaternary ammonium-based polyelectrolyte BBP exhibited a worm-to-globule transition in dilute conditions upon the addition of sodium dodecyl sulfate (SDS) due to the formation of polyelectrolyte−surfactant complexes (Figure 4e,f).[56] After the addition of α- or β-cyclodextrin, which can form an inclusion complex with SDS, the brushes switched back to the wormlike state; the BBP collapsed into a globular state again when a more competitive inclusion agent, 1-adamantylammonium chloride, was used. However, it should be noted here that the BBP concentration had to be very low; at a slightly higher concentration (e.g., 1 mg/mL), the BBP precipitated out immediately after SDS was added. Intriguingly, Gunari et al. observed that a BBP with poly(L-lysine) (PLL) side chains changed from a cylindrical to a helical conformation with a pitch of 14−24 nm before collapsing into a globular state in aqueous solutions with the increase of the amount of SDS (Figure 1k).[22] Circular dichroism measurements showed that the complexation of PLL side chains with SDS induced the formation of β-sheets on the level of a few nanometers, forcing the main chain to adopt a helical conformation on the length scale of several tens of nanometers. They further showed that the helix formation of the BBP depended on the type of surfactants, addition of salts, and pH.[57] The alkyl tail length of the surfactants was found to play a critical role; helical structures were observed only when the alkyl tail contained 10, 11, and 12 carbon atoms.[57] Addition of salts such as NaCl destroyed the helical structures as did pH conditions below 4 and above 6, presumably caused by the disintegration of BBP−surfactant complexes.

Oppositely charged polymers are known to form interpolyelectrolyte complexes (IPECs), driven by the entropic gain through the release of counterions into the bulk solution. Xu et al. reported that the quaternized BBP-D changed from wormlike to intermediate pearl-necklace and globular conformations in dilute conditions with the increase of the number of short linear poly(sodium styrenesulfonate) (PSSNa) chains.[54] In contrast, addition of long PSSNa chains collapsed the brushes into the globular state directly. Molecular dynamics simulations showed that the IPECs of the BBP and the oppositely charged linear polyelectrolyte spontaneously adopted the shape of a necklace of complex coacervate pearls formed by the complexation, and each pearl was decorated and stabilized by the uncomplexed side chains.[69]

If the backbone of BBPs is a conjugated polymer, the stimuli-induced collapse of polymeric side chains can modulate the electronic structure of the backbone, resulting in changes in the optical property, which could be employed for sensing.[70−75] Using the ATRP grafting from approach, Balamurugan et al. and Wang et al. synthesized thermoresponsive PNIPAM-grafted (PT-*g*-PNIPAM) and pH-responsive PDMAEMA-grafted polythiophene BBPs (PT-*g*-PDMA), respectively;[70,71] noticeable shifts in the absorption wavelength of the polythiophene backbone were observed when external stimuli were applied to expand or shrink the side chains. For example, Wang et al. reported that PT-*g*-PDMA in water showed a red shift of 18 nm in the maximal absorption ($\lambda_{max,abs}$) when the solution pH was decreased from 8 to 2 (Figure 5a,b) and the color of the solution changed from yellow to dark orange (Figure 5c).[71] The protonation of PDMAEMA side chains stretched the backbone and made it less folded and twisted at pH 2 than at pH 8, resulting in an increase in the conjugation length and a red shift of $\lambda_{max,abs}$. Note that PDMAEMA is soluble in water at pH 8; the shrinking of the brushes was caused by the reduced electrostatic repulsive interactions at pH 8 compared with at pH 2 and the hydrophobic polythiophene backbone. However, the experimental study of the conformational changes was obscured by the aggregation of the PT-*g*-PDMA brushes at pH 8 as revealed in the AFM experiments.[71] For the PT-*g*-PNIPAM brushes, even at a concentration of 0.8 mg/mL, the aqueous solution turned cloudy upon heating above the LCST of PNIPAM.[70]

Stimuli-responsive BBPs with a single type of homopolymer or random copolymer side chains exhibit interesting conformational transitions in response to environmental changes. However, the shape changes can only be observed at interfaces or in solutions with rather low brush concentrations, typically from tens of μg/mL to sub-mg/mL; the collapsed globular brushes are not stable and undergo aggregation and precip-

https://doi.org/10.1021/acs.jpcb.1c01819
J. Phys. Chem. B 2021, 125, 6373−6389

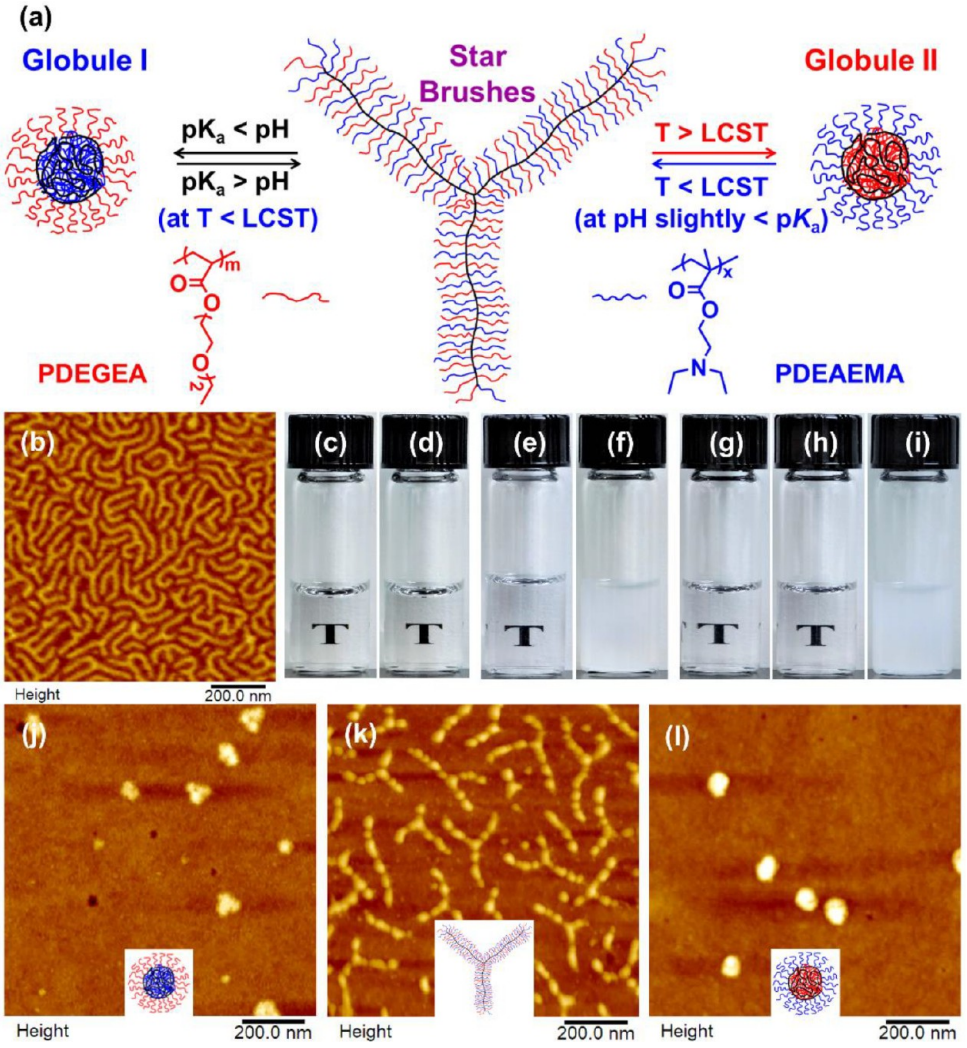

Figure 6. Stimuli-induced star−globule shape transitions of a three-arm star-shaped binary heterografted BBP composed of PDEGEA and PDEAEMA side chains (SBB-TP). (a) Schematic illustration of pH-induced and thermally induced star−globule shape transitions of SBB-TP. (b) AFM height image of SBB-TP spin-cast on mica from THF. (c−i) Optical images of 1.0 mg/g aqueous solutions of SBB-TP under various conditions: (c) pH = 5.00, T = 0 °C; (d) pH = 5.00, T = 22 °C; (e) pH = 9.50, T = 0 °C; (f) pH = 9.50, T = 22 °C; (g) pH = 7.43, T = 0 °C; (h) pH = 7.43, T = 22 °C; (i) pH = 7.43, T = 35 °C. (j−l) AFM height image of SBB-TP from a buffer solution with pH = 9.50 and T = 0 °C (j), pH = 6.60 and T = 0 °C (k), and pH = 7.43 and T = 22 °C (l). Reprinted and adapted with permission from ref 80. Copyright 2019 American Chemical Society.

itation readily, which is undesired for practical uses of stimuli-responsive shape-changing BBPs.

STIMULI-INDUCED SHAPE TRANSITIONS OF MULTICOMPONENT BBPS

To stabilize collapsed globular brushes in solution, a second, soluble polymer can be introduced into the side chains, either as a different type of side chains or as the outer block of block copolymer side chains in BBPs. When the stimuli-responsive side chains or the inner blocks become insoluble and associate into a solvophobic core, the brushes collapse into a compact structure with soluble side chains or outer blocks forming the corona. Thus, the shape transition is accompanied by the formation of stable unimolecular core−shell micelles. This concept can be extended to ternary or other multicomponent BBPs, allowing for the formation of more sophisticated morphologies. Note that multicomponent BBPs here refer to the BBPs comprising a block copolymer or two or more different types of polymers as side chains.

Stimuli-Induced Shape Transitions of Binary Heterografted BBPs with Two Types of Side Chains in Solution. PEO is a water-soluble polymer well-suited for being used as stabilizing side chains for collapsed heterografted stimuli-responsive BBPs. Henn et al. synthesized a linear heterografted BBP with a σ_{SC} of 74.3% by simultaneously clicking alkyne-end-functionalized 2 kDa PEO and thermoresponsive poly(ethoxydi(ethylene glycol)acrylate) (PDEGEA) (Scheme 1e) with a DP of 46 onto an azide-bearing backbone polymer with a DP of 800.[76] PDEGEA is a thermoresponsive polymer with an LCST of 9 °C in water.[77] A homografted PDEGEA BBP with a similar σ_{SC} was also prepared for comparison. The stabilization effect of PEO side chains for the collapsed brushes can be readily seen by warming up 1.0 mg/g aqueous solutions of the two BBPs from 0 °C. Both solutions were totally clear at 0 °C. Upon warming to 22 °C, the homografted PDEGEA BBP solution turned cloudy, while the heterografted BBP solution remained clear. DLS showed that the PEO/PDEGEA BBP exhibited a size decrease from 63 nm at 1 °C to 43 nm at 25 °C. In addition, the D_h values at 0.2 and 1.0 mg/g at 25 °C were identical, with the

https://doi.org/10.1021/acs.jpcb.1c01819
J. Phys. Chem. B 2021, 125, 6373−6389

size distributions overlapping with each other, suggesting a unimolecular collapse. AFM confirmed the heating-induced worm-to-globule shape transition.[76] Henn et al. also demonstrated the stabilization of collapsed light-responsive BBPs by PEO side chains and the UV-triggered globule-to-worm transition.[52]

Using a combination of "grafting from" and "grafting to" methods, Luo et al. synthesized a series of amphiphilic BBPs with an N_{bb} of 500, composed of PEO with a DP of 16 and poly(D,L-lactide) (PLA) of various lengths as side chains, and studied their self-assembled morphologies after a rapid change in solvent quality.[78] A multi-inlet vortex mixer was used, which allowed for micromixing of water, a selective solvent for PEO, and tetrahydrofuran, a good solvent for both, to occur in the millisecond range, enabling a homogeneous environment for self-assembly. For the BBP with a PLA DP of 11, unimolecular spherical micelles stabilized by PEO side chains were observed. With the increase of the PLA length, rods and toroids were observed, which were formed by intermolecular aggregation. They further prepared a PEO/PLA BBP with an N_{bb} of 721, an N_{PEO} of 45, and an N_{PLA} of 15. The BBP exhibited an elongated character in water, even after the collapse of PLA side chains.[23] Intriguingly, the addition of hydrophobic solutes induced the BBP to change to unimolecular spherical nanoparticles. If 5 kDa PEO was used, the solute-induced morphological transition was effectively prevented, underscoring the importance of the side chain lengths in the solution behavior of multicomponent BBPs.[79]

The stabilizing side chains can also be stimuli-responsive. The use of different stimuli-responsive polymers as side chains in the heterografted BBPs allows for attaining two or more distinct globular states from one BBP (Figure 6). Kent and Zhao prepared a three-arm star BBP (SBB-TP) composed of thermoresponsive PDEGEA and pH-responsive PDEAEMA side chains by a click "grafting to" method (Figure 6a),[80] which was confirmed by AFM (Figure 6b). The responsive behavior of 1.0 mg/g SBB-TP in buffers was visually examined first. At pH 5.00 and 0 °C, the solution was clear; upon heating to 22 °C, the solution stayed clear (Figure 6c,d), indicating the stabilization of SBB-TP by charged PDEAEMA. When PDEAEMA became insoluble at pH = 9.50, SBB-TP was stabilized by PDEGEA (Figure 6e). Heating to 22 °C caused the sample to turn cloudy due to the LCST transition of PDEGEA (Figure 6f). DLS showed that the D_h of SBB-TP at 1 °C decreased from 84.0 to 51.4 nm upon decreasing pH from 5.00 to 9.40, and no aggregation was seen at higher pH. AFM revealed that the SBB-TP from a pH 6.60 buffer at 0 °C was in a star shape but with a pearl-necklace structure (Figure 6k), presumably caused by the microphase separation of two side chain polymers along the brush backbone. At pH 9.50 and 0 °C, the brushes became globular (Figure 6j); the collapsed arms of some molecules formed three tightly associated lobes. Unexpectedly, DLS showed that at pH 5.00 the D_h did not decrease upon heating, likely due to the strong solvation of charged PDEAEMA. The pH was then increased to 7.43 to weaken the solvation, and a size transition was seen when the temperature was >15 °C. Further heating to >22 °C, however, resulted in aggregation due to the LCST transition of partially charged PDEAEMA (Figure 6g–i). The globular shape at 22 °C was verified by AFM (Figure 6l).

Kent et al. further prepared two tertiary amine-containing heterografted star BBPs composed of 5 kDa PEO and either PDMAEMA (SBB-DM) or PDEAEMA side chains (SBB-DE).[81] While SBB-DM exhibited a small size decrease and no shape transition with increasing pH from acidic to basic, a star-to-globule shape transition was observed for SBB-DE along with a large and abrupt size decrease, as expected. More intriguingly, both BBPs showed star-to-globule shape transitions in acidic solutions in response to the addition of salts containing sufficiently strong chaotropic anions (CAs) (e.g., ClO_4^-).[81] Typically, CAs have a large size and a relatively low charge density, making the water molecules surrounding them less hydrogen bonded than bulk water and thus more "chaotic".[82,83] Moreover, super-CAs such as $Fe(CN)_6^{3-}$ and $S_2O_8^{2-}$ are significantly more efficient in collapsing the star BBPs into a globular shape stabilized by PEO side chains. The shape transitions resulted from the formation of tight ion pairs of CAs and protonated tertiary amine groups and the high tendency of CAs to associate with hydrophobic groups of BBPs, which release the water molecules surrounding them into bulk water to form stronger water−water interactions and significantly decreased the solubility of the protonated tertiary amine side chains.

As shown in Figure 6k, SBB-TP exhibited a pearl-necklace morphology, similar to that of the BBPs with PAA-*b*-P*n*BA side chains in the presence of Cd^{2+} ions (Figure 1f).[11] Suspecting that the beads were formed from microphase separation of protonated PDEAEMA and PDEGEA side chains along the backbone, Kent et al. investigated the effect of buffer anions on the pearl-necklace morphology of a linear BBP composed of PDEAEMA and PDEGEA side chains in the pH 6.50 aqueous buffers at 0 °C.[18] Three buffer anions were studied: acetate carrying a charge of 1−, phosphate anions carrying charges of 2− and 1−, and citrate anions bearing charges of 3− and 2−, at pH = 6.50. Pearl-necklace nanostructures were observed for the BBP from all three aqueous buffers when spin-cast at pH 6.50 and 0 °C (Figure 1g for phosphate anions).[18] The average length of the brush molecules and the number of beads per brush decreased with increasing valency of buffer anions while the size and height of the beads increased. This indicated that multivalent anions likely formed bridges between protonated pendant tertiary amine groups and enhanced the microphase separation of two side chain polymers along the backbone.

With the introduction of a second, solvophilic polymer into side chains, collapsed BBPs were shown to be stabilized at the concentration level of ∼1.0 mg/g. For practical uses of shape-changing BBPs, it is highly desired that the unimolecular shape changing of BBPs can be achieved at higher concentrations. The shape transition of BBPs is believed to start from the collapse of side chains, followed by the coiling of the backbone to minimize the contacts of the collapsed side chains with the solvent and the transformation of the brushes into a globular shape. On the basis of this reasoning, it is possible that unimolecular shape transitions of BBPs can be achieved in moderately concentrated solutions if the thermoresponsive side chains are well-shielded from other brushes by longer protective side chains. To test this hypothesis, Henn et al. synthesized BBP-5k composed of a 5 kDa PEO (DP = 114) and a thermoresponsive, cinnamate-containing copolymer with a DP of 43 as side chains.[20] The cinnamate groups were incorporated for UV-cross-linking of the collapsed core to fix the shape at temperatures above the LCST for AFM and DLS studies at a lower temperature and after dilution. For comparison, BBP-2k and BBP-750 were synthesized using the same thermoresponsive UV-cross-linkable polymer but at 2 kDa and 750 Da PEO, respectively.

The 10 mg/g aqueous solutions of BBP-5k, -2k, and 750 were all clear at 0 °C. Upon heating, the BBP-750 solution turned

https://doi.org/10.1021/acs.jpcb.1c01819
J. Phys. Chem. B 2021, 125, 6373−6389

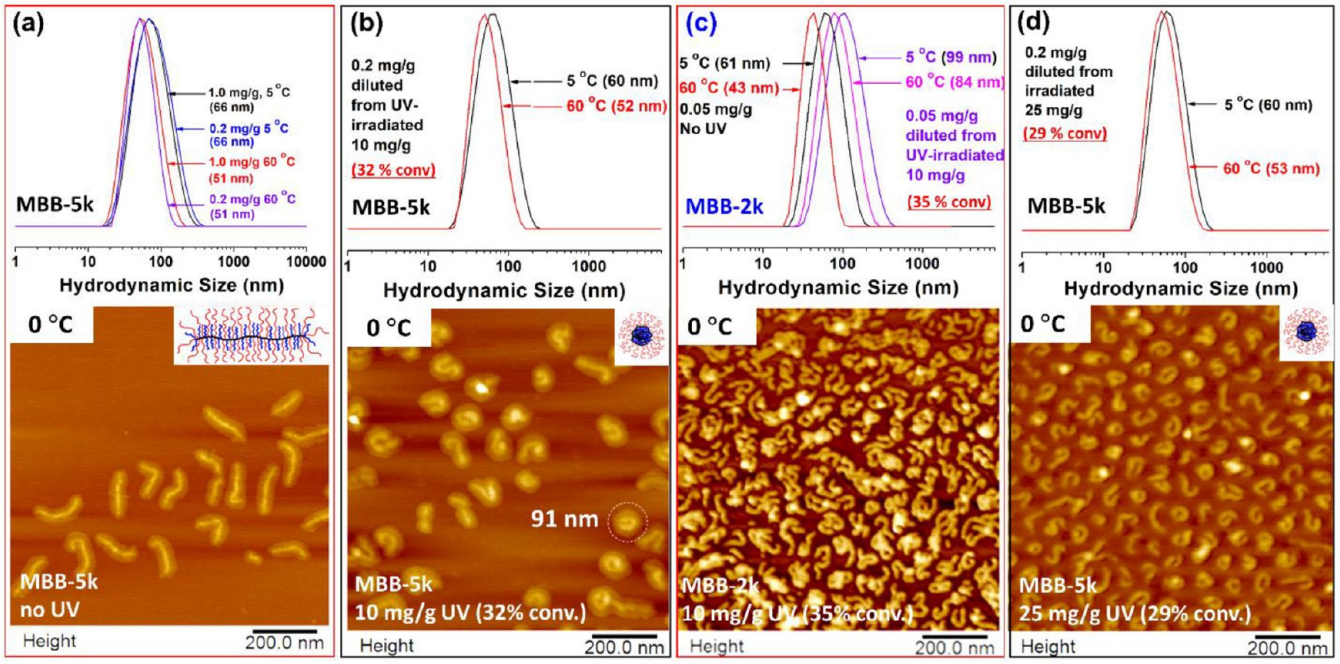

Figure 7. DLS data and AFM images on bare mica for BBP-5k and -2k: (a) nonirradiated BBP-5k; (b–d) diluted from the 10 mg/g BBP-5k solution (b), 10 mg/g MBB-2k solution (c), and 25 mg/g BBP-5k solution (d) after UV irradiation. BBP-5k: N_{bb} = 707, DP_{PEO} = 114, DP = 43 for the thermoresponsive UV-cross-linkable polymer, σ_{SC} = 87.6%. BBP-2k: DP_{PEO} = 45, σ_{SC} = 82.7%. The molar ratio of PEO to thermoresponsive UV-cross-linkable polymer in both BBPs was 0.52:0.48. Reprinted and adapted with permission from ref 20. Copyright 2018 American Chemical Society.

cloudy, indicating that the short PEO could not stabilize the collapsed brushes, while the BBP-5k and -2k solutions remained clear.[20] These two brush solutions were then irradiated at 60 °C (above the LCST) until the cinnamate conversion reached 32–35%. Unlike the wormlike morphology at 0 °C before UV irradiation (Figure 7a), most of the BBP-5k molecules were roughly spherical and well-separated at 0 °C (Figure 7b); the corona and coiled backbone can be clearly seen. After diluted to 0.2 mg/g, the D_h values of BBP-5k at 5 and 60 °C were 60 and 52 nm, respectively (Figure 7b), the same as those of the irradiated, 0.2 mg/g BBP-5k. In contrast, the irradiated BBP-2k clumped together, and the D_h values were larger at both 5 and 60 °C (Figure 7c). The BBP-5k concentration was further increased to 25 and 100 mg/g, and solutions were irradiated. For the 25 mg/g solution, single size distributions were seen at 5 and 60 °C after dilution, with essentially the same D_h values as in Figure 7b. Most of the cross-linked brushes were globular (Figure 7d), and there was no intermolecular cross-linking. For the 100 mg/g solution, an overwhelming majority of the brushes collapsed unimolecularly as seen from AFM.[20] A few molecules might be intermolecularly cross-linked, but it was also possible that they stacked on each other. By examining the AFM images, at least 95% molecules underwent a unimolecular shape transition. Although progress has been made, it remains unclear how high the brush concentration can be and whether the concentration can exceed the overlap concentration of the BBP in the solution while maintaining a unimolecular shape transition upon heating. In addition, for all of the binary heterografted BBPs studied so far, the molar ratio of two side chain polymers was ~1:1. There has been no systematic study on the effect of the molar ratio of two side chain polymers on the shape transition and the stabilization of heterografted BBPs.

Stimuli-Induced Shape Transitions of Homografted BBPs with Diblock Copolymer Side Chains in Solution. The stabilization of collapsed brushes can also be achieved by introducing a soluble polymer as the outer block of block copolymer side chains. If the outer block is also stimuli-responsive, it can provide another level of control over the behavior of BBPs in solution. Using an ATRP "grafting from" method, Yamamoto et al. synthesized a doubly thermosensitive BBP with diblock copolymer side chains composed of poly(di(ethylene glycol) methyl ether methacrylate) ($PMEO_2MA$) as the inner block and poly(tri(ethylene glycol) methyl ether methacrylate) ($PMEO_3MA$) as the outer block.[84] The LCSTs of $PMEO_2MA$ and $PMEO_2MA$ in water are 26 and 51 °C, respectively.[84−86] Transmittance and DLS studies showed the stabilization of collapsed $PMEO_2MA$ inner blocks by the outer $PMEO_3MA$ blocks upon heating.[84] Kent et al. synthesized a dually pH- and thermoresponsive BBP with PDEAEMA-*b*-poly(methoxytri(ethylene glycol) acrylate) (PTEGMA) side chains (BBP-DB), where PDEAEMA was the inner block, by a click grafting to method using an azide-functionalized backbone polymer with a DP of 707.[53] Note that the LCST of PTEGMA is 58 °C in water.[77] A 1.0 mg/g solution of BBP-DB was made and observed to remain clear when the pH was raised to 9.54 at 21 °C, at which PDEAEMA became water-insoluble while PTEGMA was soluble. Upon heating to 65 °C at pH = 9.54, the BBP-DB solution turned cloudy due to the LCST transition of the PTEGMA block. In contrast, a 0.5 mg/g solution of a BBP with only PDEAEMA side chains exhibited a clear-to-cloudy transition at room temperature when the pH was raised to above 7.3. Clearly, the PTEGMA block stabilized the collapsed BBP-DB at higher pH values, which was further confirmed by DLS. AFM showed that the BBP-DB was cylindrical at pH = 5.00 and collapsed into globules at pH = 9.56 at room temperature. When the 0.1 mg/g sample with pH of 9.54 was heated to 65 °C, the collapsed BBP-DB became more spherical. For the BBP-DB solution with a concentration of 1.0 mg/g heated to 65 °C, AFM revealed large tight clusters from the aggregation of collapsed brushes as well as individual

https://doi.org/10.1021/acs.jpcb.1c01819
J. Phys. Chem. B 2021, 125, 6373−6389

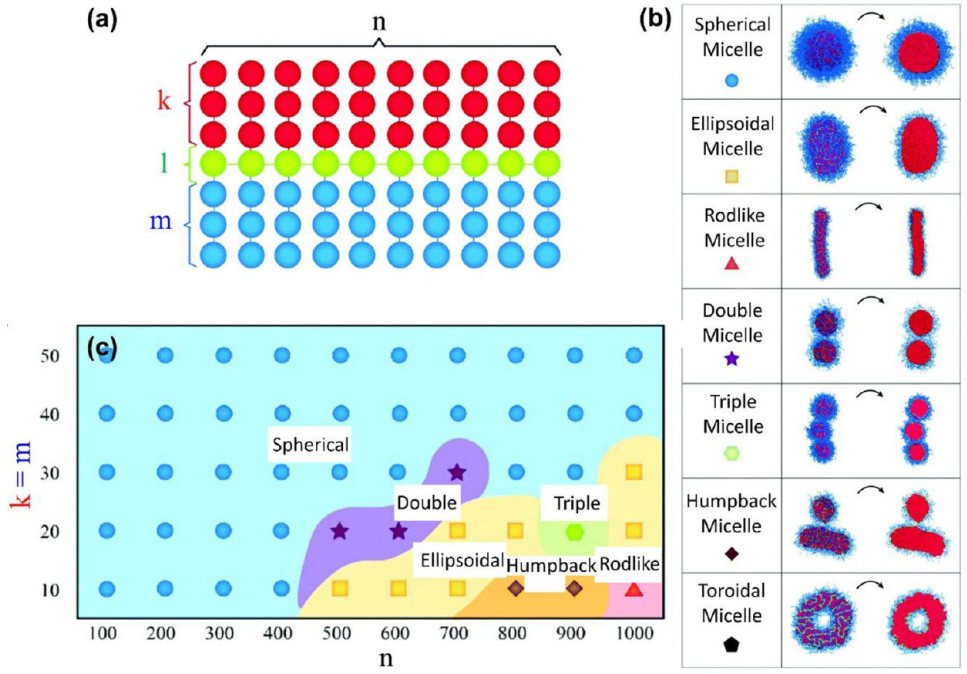

Figure 8. (a) Schematic representation of the mikto-grafted BBP composed of n macromonomer. Each macromonomer is a linear triblock oligomer $A_kC_lB_m$, where the subscripts represent the number of beads that each block is composed of and l is fixed at 1, A is the solvophobic molecular units (red), B is the solvophilic units (blue), and C is the slightly solvophobic backbone molecular units (green). (b) Various single molecule self-assembled nanostructures of the BBPs obtained after a fast quench into a bad solvent condition for A; the image on the right is a cross-section of the image on the left. (c) Morphology diagram for symmetric ($k = m$) BBPs in the parameter space (n, k) for strong incompatibility. Reprinted and adapted with permission from ref 93. Copyright 2020 Royal Society of Chemistry.

spherical nano-objects. These studies showed the stabilization of the collapsed BBPs by a soluble polymer as the outer block of diblock copolymer side chains and another level of control of the solution behavior of BBPs with the use of a stimuli-responsive polymer as the outer block. However, the effect of block lengths on the shape transition and stabilization of BBPs has not been studied.

CHALLENGES AND OUTLOOK IN THE DESIGN, SYNTHESIS, CHARACTERIZATION, AND APPLICATIONS OF STIMULI-RESPONSIVE SHAPE-CHANGING BBPS

Shape-changing BBPs not only are interesting because of their stimuli-responsive behavior but also have potential in a variety of applications. However, there are many challenges in the design, synthesis, characterization, and use of shape-changing BBPs.

(i) Guidelines are much needed for the design of multi-component shape-changing BBPs. Earlier work showed that there existed a threshold value for N_{SC} and σ_{SC} for homografted P*n*BA BBPs, below which no worm-to-sphere shape transition was observed on the water surface.[19,21] It is unclear if these empirical rules are applicable to stimuli-responsive BBPs in solution. It is also unknown whether and how N_{BB}, N_{SC}, and σ_{SC} are coupled to influence the shape-changing behavior. As a rule of thumb, longer side chains and a greater grafting density facilitate the shape changing of BBPs. For bicomponent BBPs, more molecular parameters come into play, including the length of each side chain polymer or block, grafting densities and distribution of different types of side chains in heterografted brushes, and interactions between different types of side chains or blocks and between different side chain polymers and solvent. For the worm-to-globule shape transition, the ΔG_{total} is the sum of ΔG for core ($\Delta G_{sc,core}$) and corona ($\Delta G_{sc,corona}$) formation, backbone relaxation (ΔG_{bb}), and core−water interface ($\Delta G_{interface}$). While $\Delta G_{sc,core}$ and $\Delta G_{bb} < 0$, $\Delta G_{sc,corona}$ is slightly positive because the protective side chains become more crowded. $\Delta G_{interface}$ is >0 and decreases with decreasing interfacial area. The presence of solvophilic side chains could affect the shape-changing ability. For example, Kent and Zhao observed that, when pH-responsive side chains were highly hydrated at lower pH values, the dually pH-reponsive and thermoresponsive star BBP (SBB-TP) did not exhibit a thermally induced shape transition even if the thermoresponsive side chains collapsed.[80] The situation may be even more severe for BBPs with block copolymer side chains, where the highly hydrated outer block could prevent the collapse of the inner block as observed in the particle brushes.[87] The lack of understanding of how these parameters interplay with each other in determining the dramatic shape transition of BBPs has made the design of shape-changing BBPs largely based on trial and error. Computer simulations have been performed to investigate the effects of various parameters on the morphologies of single bicomponent BBPs.[88−94] Gumus et al. recently reported an exciting simulation study of single molecule self-assembly of linear BBPs with binary mikto-grafted side chains (Figure 8a) when the solvent quality for one type of side chains was rapidly quenched from good to bad.[93] Extensive molecular dynamics simulations were performed to systematically study the influences of various molecular parameters, the degree of incompatibility between solvophilic and

https://doi.org/10.1021/acs.jpcb.1c01819
J. Phys. Chem. B 2021, 125, 6373−6389

solvophobic side chains, and the solvent quality in the low concentration limit. A variety of kinetically arrested self-assembled single brush nanostructures were observed, including unimolecular spherical, ellipsoidal, rodlike, double, triple, humpback, and toroidal micelles (Figure 8b), which were determined by the interplay between various parameters (Figure 8c). These simulation results provide qualitative guidelines for the design of shape-changing BBPs in terms of N_{BB}, N_{SC1}, and N_{SC2}, although the morphologies observed here were not thermodynamic equilibrium structures but were from rapid quenching of the solvent quality for one type of side chains; the grafting density, another critical parameter, was not taken into consideration. It represents an important step toward the rational design of shape-changing BBPs. Gumerov and Potemkin very recently conducted simulations on the BBPs composed of diblock copolymer side chains with an inner responsive block and an outer soluble block.[94] The effects of σ_{SC} and block lengths were examined, and worm-to-sphere (i.e., unimolecular spherical micelle) transitions were observed upon decreasing the solvent quality for the inner block. For BBPs with a longer outer soluble block, the association of the inner blocks becomes more difficult and occurs at poorer solvent conditions. Despite the progress, more effort is still needed to further understand the coupled influences of various molecular parameters on the transitions of multicomponent BBPs between different conformations or morphologies.

(ii) Almost all explicit dramatic shape transitions, such as wormlike/starlike-to-globular, reported in the literature so far are achieved with the use of the BBPs made from a flexible poly(meth)acrylate backbone. Stimuli-responsive BBPs composed of a conjugated polymer backbone, e.g., polythiophene, and responsive polymeric side chains have been reported;[70−75] although worm-to-globule shape transitions were proposed for the brushes to respond to environmental stimuli, the experimental verification was complicated by the intermolecular aggregation of brush molecules.[71] If the worm/rod-to-globule shape transition is unequivocally confirmed by AFM or TEM, the family of stimuli-responsive shape-changing polymers would be greatly expanded.

(iii) Synthesis of well-defined BBPs with multicomponent side chains remains a challenge. Although grafting from is suitable for the synthesis of BBPs with block copolymer side chains,[11] low initiating efficiencies have been reported, which could be exacerbated for the synthesis of stimuli-responsive BBPs that usually contain polar groups.[26] Thus, characterization of the BBPs' grafting density and block lengths is difficult. Grafting to is a modular approach, particularly suited for the preparation of multicomponent heterografted BBPs. However, the removal of unreacted side chains can be laborious. Usually, multiple rounds of fractionation and centrifugal filtration are performed to purify the BBPs.[20,76,80] More efficient, clean synthetic methods for the synthesis of multicomponent stimuli-responsive shape-changing BBPs are much needed.

(iv) Although shape transitions of linear P*n*BA BBPs have been observed in situ by AFM in the environmental chamber upon changing solvent vapors, direct imaging of the entire shape-changing process in solution by a microscopy method has not been reported. Note that Li et al. reported the conformations of PNIPAM BBPs in water in a fluidic cell at two different temperatures but not the whole process.[36] With the advance of microscopy techniques, it is possible to achieve this, e.g., by using liquid phase TEM or AFM,[95,96] which could also help clarify if it is possible to realize single molecule shape transitions of BBPs in moderately concentrated solutions.

(v) Long linear flexible polymer molecules are known to undergo coil−stretch transitions in dilute conditions when subjected to an elongational flow, which have been intensively studied, theoretically and experimentally.[97−100] The shape changing of single linear polymer chains from a coiled to an elongated state occurs when the strain rate exceeds a threshold value at which the shear force becomes greater than the entropic retraction force. It would be highly interesting to investigate the possible shear-induced shape-changing behavior of collapsed globular stimuli-responsive BBPs in extensional flow.

(vi) Current study of shape-changing BBPs has been focused on the single brush molecules. Is it possible to design stimuli-responsive systems that can translate shape transitions at the molecular level to macroscopic shape shifting? At present, shape-shifting meso- and macroscopic objects are largely fabricated by top-down approaches.[101] It would be exciting if such systems can be achieved through bottom-up approaches using nanoscale shape-changing BBPs.

(vii) Shape-changing BBPs have potential applications in many areas, but there are few demonstrations. As mentioned earlier, Luo et al. reported hydrophobic solute-induced worm-to-sphere morphological transitions of amphiphilic BBPs,[23] which may find applications in drug loading and delivery. Henn et al., on the other hand, showed that the shape transitions of BBPs can be utilized to regulate molecular binding.[76] If functional groups are incorporated into the core-forming side chains, they would not be accessible in the globular state to the molecules in the surrounding environment but become accessible in the wormlike state, which could be used to mimic the function of certain proteins.[102] Henn et al. prepared a BBP composed of a PEO and a biotin- and fluorescence dye-containing thermoresponsive polymer as side chains and used the fluorescence resonance energy transfer (FRET) technique to study the binding of this BBP with rhodamine B-labeled avidin.[76] At 40 °C when the BBP was in a globular state, little FRET was observed. However, when the temperature was lowered to 0 °C, the BBP was unfolded to the wormlike state and the FRET increased significantly, suggesting the binding of biotin and avidin. No example has been reported yet on the use of shape-changing BBPs in the design of responsive catalysts. Plenty of opportunities could be envisioned for potential applications of stimuli-responsive shape-changing BBPs.

SUMMARY

BBPs have been shown to exhibit different morphologies under different conditions and can be induced to change from one shape to another using external stimuli. The dramatic shape transitions of BBPs with a single type of homopolymer or random copolymer side chains have been demonstrated by lateral compression on the water surface, treatment with

https://doi.org/10.1021/acs.jpcb.1c01819
J. Phys. Chem. B 2021, 125, 6373−6389

different solvent vapors on solid substrates, and application of external stimuli in solutions. However, the collapsed BBPs are unstable and prone to aggregation. The collapsed globular brushes can be stabilized by introducing a second, solvophilic polymer into the side chains, either as a distinct type of side chains or as the outer block of block copolymer side chains. In addition, if the protective side chains are significantly longer than that of stimuli-responsive side chains, unimolecular shape transitions are possible in moderately concentrated aqueous solutions, although the issue is not fully understood. While much progress has been achieved, many challenges remains in the design, synthesis, characterization, understanding, and applications of stimuli-responsive shape-changing BBPs. Despite these challenges, it is believed that exciting advances will be seen in every aspect of shape-changing BBPs in near future.

AUTHOR INFORMATION

Corresponding Author

Bin Zhao − *Department of Chemistry, University of Tennessee, Knoxville, Tennessee 37996, United States;* orcid.org/0000-0001-5505-9390; Email: bzhao@utk.edu

Complete contact information is available at: https://pubs.acs.org/10.1021/acs.jpcb.1c01819

Notes

The author declares no competing financial interest.

Biography

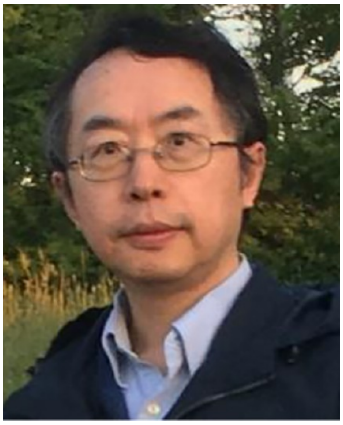

Bin Zhao received his Ph.D. degree in polymer science from the University of Akron in 2000. After a postdoctoral stint at the University of Illinois at Urbana−Champaign, he started his independent career in 2002. Currently, he is Paul and Wilma Ziegler Professor in the Department of Chemistry at the University of Tennessee, Knoxville. His research interests include macromolecular brush materials, stimuli-responsive polymers, and liquid crystalline polymers.

ACKNOWLEDGMENTS

B.Z. thanks NSF for the support of his research on bottlebrush polymers (DMR-1607076 and -2004564).

REFERENCES

(1) Zhang, M. F.; Müller, A. H. E. Cylindrical Polymer Brushes. *J. Polym. Sci., Part A: Polym. Chem.* **2005**, *43*, 3461−3481.

(2) Yuan, J. Y.; Muller, A. H. E.; Matyjaszewski, K.; Sheiko, S. S. Molecular Brushes. In *Polymer Science: A Comprehensive Reference, 10 Vol. Set*; Elsevier, 2012; Vol. *6*, pp 199−264.

(3) Sheiko, S. S.; Sumerlin, B. S.; Matyjaszewski, K. Cylindrical Molecular Brushes: Synthesis, Characterization, and Properties. *Prog. Polym. Sci.* **2008**, *33*, 759−785.

(4) Lee, H.-I.; Pietrasik, J.; Sheiko, S. S.; Matyjaszewski, K. Stimuli-Responsive Molecular Brushes. *Prog. Polym. Sci.* **2010**, *35*, 24−44.

(5) Xie, G.; Martinez, M. R.; Olszewski, M.; Sheiko, S. S.; Matyjaszewski, K. Molecular Bottlebrushes as Novel Materials. *Biomacromolecules* **2019**, *20*, 27−54.

(6) Daniel, W. F.; Burdynska, J.; Vatankhah-Varnoosfaderani, M.; Matyjaszewski, K.; Paturej, J.; Rubinstein, M.; Dobrynin, A. V.; Sheiko, S. S. Solvent-Free, Supersoft and Superelastic Bottlebrush Melts and Networks. *Nat. Mater.* **2016**, *15*, 183−189.

(7) Qi, H.; Liu, X. T.; Henn, D. M.; Mei, S.; Staub, M. C.; Zhao, B.; Li, C. Y. Breaking Translational Symmetry via Polymer Chain Overcrowding in Molecular Bottlebrush Crystallization. *Nat. Commun.* **2020**, *11*, 2152.

(8) Liberman-Martin, A. L.; Chu, C. K.; Grubbs, R. H. Application of Bottlebrush Block Copolymers as Photonic Crystals. *Macromol. Rapid Commun.* **2017**, *38*, 1700058.

(9) Banquy, X.; Burdyńska, J.; Lee, D. W.; Matyjaszewski, K.; Israelachvili, J. Bioinspired Bottle-Brush Polymer Exhibits Low Friction and Amontons-like Behavior. *J. Am. Chem. Soc.* **2014**, *136*, 6199−6202.

(10) Johnson, J. A.; Lu, Y. Y.; Burts, A. O.; Xia, Y.; Durrell, A. C.; Tirrell, D. A.; Grubbs, R. H. Drug-Loaded, Bivalent-Bottle-Brush Polymers by Graft-through ROMP. *Macromolecules* **2010**, *43*, 10326−10335.

(11) Zhang, M.; Drechsler, M.; Müller, A. H. E. Template-Controlled Synthesis of Wire-Like Cadmium Sulfide Nanoparticle Assemblies within Core-Shell Cylindrical Polymer Brushes. *Chem. Mater.* **2004**, *16*, 537−543.

(12) Chancellor, A. J.; Seymour, B. T.; Zhao, B. Characterizing Polymer-Grafted Nanoparticles: From Basic Defining Parameters to Behavior in Solvents and Self-Assembled Structures. *Anal. Chem.* **2019**, *91*, 6391−6402.

(13) Hiemenz, P. C.; Lodge, T. P. *Polymer Chemistry*, 2nd ed.; CRC Press: Boca Raton, FL, 2007.

(14) Sheiko, S. S.; Sun, F. C.; Randall, A.; Shirvanyants, D.; Rubinstein, M.; Lee, H.-i.; Matyjaszewski, K. Adsorption-Induced Scission of Carbon-Carbon Bonds. *Nature* **2006**, *440*, 191−194.

(15) Saariaho, M.; Subbotin, A.; Szleifer, I.; Ikkala, O.; Ten Brinke, G. Effect of Side Chain Rigidity on the Elasticity of Comb Copolymer Cylindrical Brushes: A Monte Carlo Simulation Study. *Macromolecules* **1999**, *32*, 4439.

(16) Fischer, K.; Schmidt, M. Solvent-Induced Length Variation of Cylindrical Brushes. *Macromol. Rapid Commun.* **2001**, *22*, 787−791.

(17) Potemkin, I. I.; Khokhlov, A. R.; Prokhorova, S.; Sheiko, S. S.; Moller, M.; Beers, K. L.; Matyjaszewski, K. Spontaneous Curvature of Comblike Polymers at a Flat Interface. *Macromolecules* **2004**, *37*, 3918−3923.

(18) Kent, E. W.; Lewoczko, E. M.; Zhao, B. Effect of Buffer Anions on Pearl-Necklace Morphology of Tertiary Amine-Containing Binary Heterografted Linear Molecular Bottlebrushes in Acidic Aqueous Buffers. *Langmuir* **2020**, *36*, 13320−13330.

(19) Sheiko, S. S.; Prokhorova, S. A.; Beers, K. L.; Matyjaszewski, K.; Potemkin, I. I.; Khokhlov, A. R.; Möller, M. Single Molecule Rod-Globule Phase Transition for Brush Molecules at a Flat Interface. *Macromolecules* **2001**, *34*, 8354−8360.

(20) Henn, D. M.; Holmes, J. A.; Kent, E. W.; Zhao, B. Worm-to-Sphere Shape Transition of Thermoresponsive Linear Molecular Bottlebrushes in Moderately Concentrated Aqueous Solution. *J. Phys. Chem. B* **2018**, *122*, 7015−7025.

(21) Lord, S. J.; Sheiko, S. S.; LaRue, I.; Lee, H.-I.; Matyjaszewski, K. Tadpole Conformation of Gradient Polymer Brushes. *Macromolecules* **2004**, *37*, 4235−4240.

(22) Gunari, N.; Cong, Y.; Zhang, B.; Fischer, K.; Janshoff, A.; Schmidt, M. Surfactant-Induced Helix Formation of Cylindrical Brush Polymers with Poly(*L*-lysine) Side Chains. *Macromol. Rapid Commun.* **2008**, *29*, 821−825.

(23) Luo, H.; Szymusiak, M.; Garcia, E. A.; Lock, L. L.; Cui, H.; Liu, Y.; Herrera-Alonso, M. Solute-Triggered Morphological Transitions of an Amphiphilic Heterografted Brush Copolymer as a Single-Molecule Drug Carrier. *Macromolecules* **2017**, *50*, 2201−2206.

(24) Runge, M. B.; Dutta, S.; Bowden, N. B. Synthesis of Comb Block Copolymers by ROMP, ATRP, and ROP and Their Assembly in the Solid State. *Macromolecules* **2006**, *39*, 498−508.
(25) Bolton, J.; Rzayev, J. Tandem ATRP-RAFT Synthesis of Polystyrene-Poly(Methyl Methacrylate) Bottlebrush Block Copolymers and Their Self-Assembly into Cylindrical Nanostructures. *ACS Macro Lett.* **2012**, *1*, 15−18.
(26) Xu, Y.; Bolisetty, S.; Drechsler, M.; Fang, B.; Yuan, J.; Ballauff, M.; Muller, A. X. E. pH and Salt Responsive Poly(*N*,*N*-dimethylaminoethyl methacrylate) Cylindrical Brushes and Their Quaternized Derivatives. *Polymer* **2008**, *49*, 3957−3964.
(27) Yan, Y.; Shi, Y.; Zhu, W.; Chen, Y. Highly Efficient Synthesis of Cylindrical Polymer Brushes with Various Side Chains via Click Grafting-Onto Approach. *Polymer* **2013**, *54*, 5634−5642.
(28) Han, D.; Tong, X.; Zhao, Y. One-Pot Synthesis of Brush Diblock Copolymers through Simultaneous ATRP and Click Coupling. *Macromolecules* **2011**, *44*, 5531−5536.
(29) Tsukahara, Y.; Mizuno, K.; Segawa, A.; Yamashita, Y. Study on the Radical Polymerization Behavior of Macromonomers. *Macromolecules* **1989**, *22*, 1546−1552.
(30) Xia, Y.; Olsen, B. D.; Kornfield, J. A.; Grubbs, R. H. Efficient Synthesis of Narrowly Dispersed Brush Copolymers and Study of Their Assemblies: The Importance of Side Chain Arrangement. *J. Am. Chem. Soc.* **2009**, *131*, 18525−18532.
(31) Li, Z.; Ma, J.; Cheng, C.; Zhang, K.; Wooley, K. L. Synthesis of Hetero-Grafted Amphiphilic Diblock Molecular Brushes and Their Self-Assembly in Aqueous Medium. *Macromolecules* **2010**, *43*, 1182−1184.
(32) Li, Y.; Themistou, E.; Zou, J.; Das, B. P.; Tsianou, M.; Cheng, C. Facile Synthesis and Visualization of Janus Double-Brush Copolymers. *ACS Macro Lett.* **2012**, *1*, 52−56.
(33) Ishizu, K.; Satoh, J.; Sogabe, A. Architecture and Solution Properties of AB-Type Brush-Block-Brush Amphiphilic Copolymers via ATRP Techniques. *J. Colloid Interface Sci.* **2004**, *274*, 472−479.
(34) Gallyamov, M. O.; Tartsch, B.; Khokhlov, A. R.; Sheiko, S. S.; Börner, H. G.; Matyjaszewski, K.; Möller, M. Reversible Collapse of Brushlike Macromolecules in Ethanol and Water Vapours as Revealed by Real-Time Scanning Force Microscopy. *Chem. Eur. Chem. - Eur. J.* **2004**, *10*, 4599−4605.
(35) Gallyamov, M. O.; Tartsch, B.; Khokhlov, A. R.; Sheiko, S. S.; Börner, H. G.; Matyjaszewski, K.; Möller, M. Real-Time Scanning Force Microscopy of a Macromolecular Conformational Transitions. *Macromol. Rapid Commun.* **2004**, *25*, 1703−1707.
(36) Li, C.; Gunari, N.; Fischer, K.; Janshoff, A.; Schmidt, M. New Perspectives for the Design of Molecular Actuators: Thermally Induced Collapse of Single Macromolecules from Cylindrical Brushes to Spheres. *Angew. Chem., Int. Ed.* **2004**, *43*, 1101−1104.
(37) Lee, H.-I.; Boyce, J. R.; Nese, A.; Sheiko, S. S.; Matyjaszewski, K. pH-Induced Conformational Changes of Loosely Grafted Molecular Brushes Containing Poly(acrylic acid) Side Chains. *Polymer* **2008**, *49*, 5490−5496.
(38) Boyce, J. R.; Shirvanyants, D.; Sheiko, S. S.; Ivanov, D. A.; Qin, S. H.; Börner, H.; Matyjaszewski, K. Multiarm Molecular Brushes: Effect of the Number of Arms on the Molecular Weight Polydispersity and Surface Ordering. *Langmuir* **2004**, *20*, 6005−6011.
(39) Sheiko, S. S.; Möller, M. Visualization of Macromolecules: A First Step to Manipulation and Controlled Response. *Chem. Rev.* **2001**, *101*, 4099−4123.
(40) Sun, F.; Sheiko, S. S.; Moeller, M.; Beers, K.; Matyjaszewski, K. Conformational Switching of Molecular Brushes in Response to the Energy of Interaction with the Substrate. *J. Phys. Chem. A* **2004**, *108*, 9682−9686.
(41) Gallyamov, M. O.; Tartsch, B.; Khokhlov, A. R.; Sheiko, S. S.; Borner, H. G.; Matyjaszewski, K.; Moller, M. Conformational Dynamics of Single Molecules Visualized in Real Time by Scanning Force Microscopy: Macromolecular Mobility on a Substrate Surface in Different Vapours. *J. Microsc.* **2004**, *215*, 245−256.
(42) Gallyamov, M. O.; Tartsch, B.; Mela, P.; Borner, H.; Matyjaszewski, K.; Sheiko, S.; Khokhlov, A.; M?ller, M. A Scanning Force Microscopy Study on the Motion of Single Brush-Like Macromolecules on a Silicon Substrate Induced by Coadsorption of Small Molecules. *Phys. Chem. Chem. Phys.* **2007**, *9*, 346−352.
(43) Gil, E. S.; Hudson, S. M. Stimuli-Reponsive Polymers and Their Bioconjugates. *Prog. Polym. Sci.* **2004**, *29*, 1173−1222.
(44) Zhou, K. J.; Wang, Y. G.; Huang, X. N.; Luby-Phelps, K.; Sumer, B. D.; Gao, J. M. Tunable, Ultrasensitive pH-Responsive Nanoparticles Targeting Specific Endocytic Organelles in Living Cells. *Angew. Chem., Int. Ed.* **2011**, *50*, 6109−6114.
(45) Schild, H. G. Poly(*N*-isopropylacrylamide): Experiment, Theory and Application. *Prog. Polym. Sci.* **1992**, *17*, 163−249.
(46) Lewoczko, E. M.; Wang, N.; Lundberg, C. E.; Kelly, M. T.; Kent, E. W.; Wu, T.; Chen, M.-L.; Wang, J.-H.; Zhao, B. Effects of *N*-Substituents on Solution Behavior of Poly(sulfobetaine methacrylate)s in Water: UCST and LCST. *ACS Applied Polymer Materials* **2021**, *3*, 867−878.
(47) Wang, N.; Seymour, B. T.; Lewoczko, E. M.; Kent, E. W.; Chen, M.-L.; Wang, J.-H.; Zhao, B. Zwitterionic Poly(sulfobetaine methacrylate)s in Water: From Upper Critical Solution Temperature (UCST) to Lower Critical Solution Temperature (LCST) with Increasing Length of One Alkyl Substituent on the Nitrogen Atom. *Polym. Chem.* **2018**, *9*, 5257−5261.
(48) Zhao, Y. Light-Responsive Block Copolymer Micelles. *Macromolecules* **2012**, *45*, 3647−3657.
(49) Lee, H.-I.; Pietrasik, J.; Matyjaszewski, K. Phototunable Temperature-Responsive Molecular Brushes Prepared by ATRP. *Macromolecules* **2006**, *39*, 3914−3920.
(50) Pietrasik, J.; Sumerlin, B. S.; Lee, R. Y.; Matyjaszewski, K. Solution Behavior of Temperature-Responsive Molecular Brushes Prepared by ATRP. *Macromol. Chem. Phys.* **2007**, *208*, 30−36.
(51) Yamamoto, S.-i.; Pietrasik, J.; Matyjaszewski, K. Temperature- and pH-Responsive Dense Copolymer Brushes Prepared by ATRP. *Macromolecules* **2008**, *41*, 7013−7020.
(52) Henn, D. M.; Lau, C. M.; Li, C. Y.; Zhao, B. Light-Triggered Unfolding of Single Linear Molecular Bottlebrushes from Compact Globular to Wormlike Nano-Objects in Water. *Polym. Chem.* **2017**, *8*, 2702−2712.
(53) Kent, E. W.; Henn, D. M.; Zhao, B. Shape-Changing Linear Molecular Bottlebrushes with Dually pH- and Thermo-Responsive Diblock Copolymer Side Chains. *Polym. Chem.* **2018**, *9*, 5133−5144.
(54) Xu, Y.; Borisov, O. V.; Ballauff, M.; Muller, A. H. Manipulating the Morphologies of Cylindrical Polyelectrolyte Brushes by Forming Interpolyelectrolyte Complexes with Oppositely Charged Linear Polyelectrolytes: an AFM Study. *Langmuir* **2010**, *26*, 6919−6926.
(55) Xu, Y.; Bolisetty, S.; Drechsler, M.; Fang, B.; Yuan, J.; Harnau, L.; Ballauff, M.; Müller, A. X. E. Manipulating Cylindrical Polyelectrolyte Brushes on the Nanoscale by Counterions: Collapse Transition to Helical Structures. *Soft Matter* **2009**, *5*, 379−384.
(56) Xu, Y.; Bolisetty, S.; Ballauff, M.; Müller, A. H. E. Switching the Morphologies of Cylindrical Polycation Brushes by Ionic and Supramolecular Inclusion Complexes. *J. Am. Chem. Soc.* **2009**, *131*, 1640−1641.
(57) Cong, Y.; Gunari, N.; Zhang, B.; Janshoff, A.; Schmidt, A. Hierarchical Structure Formation of Cylindrical Brush Polymer-Surfactant Complexes. *Langmuir* **2009**, *25*, 6392−6397.
(58) Stephan, T.; Muth, S.; Schmidt, M. Shape Changes of Statisical Copolymacromomers: From Wormlike Cylinders to Horseshoe- and Meanderlike Structures. *Macromolecules* **2002**, *35*, 9857−9860.
(59) Mukumoto, K.; Li, Y.; Nese, A.; Sheiko, S. S.; Matyjaszewski, K. Synthesis and Characterization of Molecular Bottlebrushes Prepared by Iron-Based ATRP. *Macromolecules* **2012**, *45*, 9243−9249.
(60) Zhang, N.; Luxenhofer, R.; Jordan, R. Thermoresponsive Poly(2-oxazoline) Molecular Brushes by Living Ionic Polymerization: Kinetic Investigations of Pendant Chain Grafting and Cloud Point Modulation by Backbone and Side Chain Length Variation. *Macromol. Chem. Phys.* **2012**, *213*, 973−981.
(61) Weller, D.; McDaniel, J. R.; Fischer, K.; Chilkoti, A.; Schmidt, M. Cylindrical Polymer Brushes with Elastin-Like Polypeptide Side Chains. *Macromolecules* **2013**, *46*, 4966−4971.

https://doi.org/10.1021/acs.jpcb.1c01819
J. Phys. Chem. B 2021, 125, 6373−6389

(62) Liu, W.; Liu, Y.; Zeng, G.; Liu, R.; Huang, Y. Coil-to-Rod Conformational Transition and Single Chain Structure of Graft Copolymer by Tuning the Graft Density. *Polymer* **2012**, *53*, 1005−1014.
(63) Kutnyanszky, E.; Hempenius, M. A.; Vancso, G. J. Polymer Bottlebrushes with a Redox Responsive Backbone Feel the Heat: Synthesis and Characterization of Dual Responsive Poly(ferrocenylsilane)s with PNIPAM Side Chains. *Polym. Chem.* **2014**, *5*, 771−783.
(64) Li, X.; ShamsiJazeyi, H.; Pesek, S. L.; Agrawal, A.; Hammouda, B.; Verduzco, R. Thermoresponsive PNIPAAM Bottlebrush Polymers with Tailored Side-Chain Length and End-Group Structure. *Soft Matter* **2014**, *10*, 2008−2015.
(65) Zhu, X. M.; Zhang, J.; Miao, C.; Li, S. Y.; Zhao, Y. L. Synthesis, Thermoresponsivity and Multi-Tunable Hierarchical Self-assembly of Multi-Responsive $(AB)_mC$ Miktobrush-Coil Terpolymers. *Polym. Chem.* **2020**, *11*, 3003−3017.
(66) Yan, Y. Y.; Gao, C.; Li, J. J.; Zhang, T.; Yang, G.; Wang, Z. K.; Hua, Z. Modulating Morphologies and Surface Properties of Nanoparticles from Cellulose-Grafted Bottlebrush Copolymers Using Complementary Hydrogen-Bonding between Nucleobases. *Biomacromolecules* **2020**, *21*, 613−620.
(67) Henn, D. M.; Wright, R. A. E.; Woodcock, J. W.; Hu, B.; Zhao, B. Tertiary Amine-Containing Thermo- and pH-Sensitive Hydrophilic ABA Triblock Copolymers: Effect of Different Tertiary Amines on Thermally Induced Sol-Gel Transitions. *Langmuir* **2014**, *30*, 2541−2550.
(68) Mori, H.; Müller, A. H. E. New Polymeric Architectures with (Meth)acrylic Acid Segments. *Prog. Polym. Sci.* **2003**, *28*, 1403−1439.
(69) Polotsky, A.; Charlaganov, M.; Xu, Y.; Leermakers, F. A. M.; Daoud, M.; Müller, A. H. E.; Dotera, T.; Borisov, O. Pearl-Necklace Structures in Core-Shell Molecular Brushes: Experiments, Monte Carlo Simulations, and Self-Consistent Field Modeling. *Macromolecules* **2008**, *41*, 4020−4028.
(70) Balamurugan, S. S.; Bantchev, G. B.; Yang, Y.; McCarley, R. L. Highly Water Soluble Thermally Responsive Poly(thiophene)-Based Brushes. *Angew. Chem., Int. Ed.* **2005**, *44*, 4872−4876.
(71) Wang, M. F.; Zou, S.; Guerin, G.; Shen, L.; Deng, K. Q.; Jones, M.; Walker, G. C.; Scholes, G. D.; Winnik, M. A. A Water-Soluble pH-Responsive Molecular Brush of Poly(*N*,*N*-dimethylaminoethyl methacrylate) Grafted Polythiophene. *Macromolecules* **2008**, *41*, 6993−7002.
(72) Choi, J. W.; Ruiz, C. R.; Nesterov, E. E. Temperature-Induced Control of Conformation and Conjugation Length in Water-Soluble Fluorescent Polythiophenes. *Macromolecules* **2010**, *43*, 1964−1974.
(73) Ghosh, R.; Chatterjee, D. P.; Das, S.; Mukhopadhyay, T. K.; Datta, A.; Nandi, A. K. Influence of Hofmeister I^- on Tuning Optoelectronic Properties of Ampholytic Polythiophene by Varying pH and Conjugating with RNA. *Langmuir* **2017**, *33*, 12739−12749.
(74) Ghosh, R.; Das, S.; Bhattacharyya, K.; Chatterjee, D. P.; Biswas, A.; Nandi, A. K. Light-Induced Conformational Change of Uracil-Anchored Polythiophene-Regulating Thermo-Responsiveness. *Langmuir* **2018**, *34*, 12401−12411.
(75) Damavandi, M.; Pilkington, L. I.; Malmström, J.; Whitehead, K. A.; Travas-Sejdic, J.; Barker, D. Poly-*p*-phenylenevinylene-*g*-poly(2-(methacryloyloxy)ethyl) trimethylammonium chloride (PPV-*g*-PMETAC): a Fluorescent, Water-Soluble, Selective Anion Sensor. *J. Polym. Sci., Part A: Polym. Chem.* **2018**, *56*, 1997−2003.
(76) Henn, D. M.; Fu, W. X.; Mei, S.; Li, C. Y.; Zhao, B. Temperature-Induced Shape Changing of Thermosensitive Binary Heterografted Linear Molecular Brushes between Extended Worm-Like and Stable Globular Conformations. *Macromolecules* **2017**, *50*, 1645−1656.
(77) Jin, N. X.; Woodcock, J. W.; Xue, C. M.; O'Lenick, T. G.; Jiang, X. G.; Jin, S.; Dadmun, M. D.; Zhao, B. Tuning of Thermo-Triggered Gel-to-Sol Transition of Aqueous Solution of Multi-Responsive Diblock Copolymer Poly(methoxytri(ethylene glycol) acrylate-*co*-acrylic acid)-*b*-poly(ethoxydi(ethylene glycol) acrylate). *Macromolecules* **2011**, *44*, 3556−3566.
(78) Luo, H. Y.; Santos, J. L.; Herrera-Alonso, M. Toroidal Structures from Brush Amphiphiles. *Chem. Commun.* **2014**, *50*, 536−538.
(79) Garcia, E. A.; Luo, H. Y.; Mack, C. E.; Herrera-Alonso, M. Effect of Side-Chain Length on Solute Encapsulation by Amphiphilic Heterografted Brush Copolymers. *Soft Matter* **2020**, *16*, 8871−8876.
(80) Kent, E. W.; Zhao, B. Stimuli-Induced Star-Globule Shape Transitions of Dually Responsive Binary Heterografted Three-Arm Star Molecular Brushes in Aqueous Solution. *Macromolecules* **2019**, *52*, 6714−6724.
(81) Kent, E. W.; Lewoczko, E. M.; Zhao, B. pH- and Chaotropic Anion-Induced Conformational Changes of Tertiary Amine-Containing Binary Heterografted Star Molecular Bottlebrushes in Aqueous Solution. *Polym. Chem.* **2021**, *12*, 265−276.
(82) Marcus, Y. Effect of Ions on the Structure of Water: Structure Making and Breaking. *Chem. Rev.* **2009**, *109*, 1346−1370.
(83) Assaf, K. I.; Nau, W. M. The Chaotropic Effect as an Assembly Motif in Chemistry. *Angew. Chem., Int. Ed.* **2018**, *57*, 13968−13981.
(84) Yamamoto, S.-i.; Pietrasik, J.; Matyjaszewski, K. ATRP Synthesis of Thermally Responsive Molecular Brushes from Oligo(ethylene oxide) Methacrylates. *Macromolecules* **2007**, *40*, 9348−9353.
(85) Horton, J. M.; Bai, Z.; Jiang, X.; Li, D.; Lodge, T. P.; Zhao, B. Spontaneous Phase Transfer of Thermosensitive Hairy Particles between Water and an Ionic Liquid. *Langmuir* **2011**, *27*, 2019−2027.
(86) Hu, B.; Fu, W. X.; Zhao, B. Enhancing Gelation of Thermosensitive Hydrophilic ABC Linear Triblock Copolymers in Water by Thermoresponsive Hairy Nanoparticles. *Macromolecules* **2016**, *49*, 5502−5513.
(87) Wright, R. A. E.; Hu, B.; Henn, D. M.; Zhao, B. Reversible Sol-Gel Transitions of Aqueous Dispersions of Silica Nanoparticles Grafted with Diblock Copolymer Brushes Composed of a Thermosensitive Inner Block and a Charged Outer Block. *Soft Matter* **2015**, *11*, 6808−6820.
(88) Theodorakis, P. E.; Paul, W.; Binder, K. Interplay between Chain Collapse and Microphase Separation in Bottle-Brush Polymers with Two Types of Side Chains. *Macromolecules* **2010**, *43*, 5137−5148.
(89) Theodorakis, P. E.; Paul, W.; Binder, K. Analysis of the Cluster Formation in Two-Component Cylindrical Bottle-brush Polymers under Poor Solvent Conditions. A Simulation Study. *Eur. Phys. J. E: Soft Matter Biol. Phys.* **2011**, *34*, 52.
(90) Erukhimovich, I.; Theodorakis, P. E.; Paul, W.; Binder, K. Mesophase Formation in Two-Component Cylindrical Bottlebrush Polymers. *J. Chem. Phys.* **2011**, *134*, 054906.
(91) Fytas, N. G.; Theodorakis, P. E. Phase Behavior of Two-Component Bottle-Brush Polymers with Flexible Backbones under Poor Solvent Conditions. *Mater. Res. Express* **2014**, *1*, 015301.
(92) Zhang, Y. C.; Xi, S.; Parambathu, A. V.; Chapman, W. G. Density Functional Study of One- and Two-Component Bottlebrush Molecules in Solvents of Varying Quality. *Mol. Phys.* **2020**, *118*, No. e1767812.
(93) Gumus, B.; Herrera-Alonso, M.; Ramírez-Hernández, A. Kinetically-Arrested Single-Polymer Nanostructures from Amphiphilic Mikto-Grafted Bottlebrushes in Solution: a Simulation Study. *Soft Matter* **2020**, *16*, 4969−4979.
(94) Gumerov, R. A.; Potemkin, I. I. Computer Simulations of Comb-Like Macromolecules with Responsive Diblock Copolymer Side Chains. *Colloid Polym. Sci.* **2021**, *299*, 407−418.
(95) Parent, L. R.; Bakalis, E.; Ramírez-Hernández, A.; Kammeyer, J. K.; Park, C.; de Pablo, J.; Zerbetto, F.; Patterson, J. P.; Gianneschi, N. C. Directly Observing Micelle Fusion and Growth in Solution by Liquid-Cell Transmission Electron Microscopy. *J. Am. Chem. Soc.* **2017**, *139*, 17140−17151.
(96) Early, J. T.; Yager, K. G.; Lodge, T. P. Direct Observation of Micelle Fragmentation via In Situ Liquid-Phase Transmission Electron Microscopy. *ACS Macro Lett.* **2020**, *9*, 756−761.
(97) de Gennes, P. G. Coil-Stretch Transition of Dilute Flexible Polymers under Ultrahigh Velocity Gradients. *J. Chem. Phys.* **1974**, *60*, 5030−5042.
(98) Larson, R. G.; Magda, J. J. Coil-Stretch Transitions in Mixed Shear and Extensional Flows of Dilute Polymer Solutions. *Macromolecules* **1989**, *22*, 3004−3010.

https://doi.org/10.1021/acs.jpcb.1c01819
J. Phys. Chem. B 2021, 125, 6373−6389

(99) Perkins, T. T.; Smith, D. E.; Chu, S. Single Polymer Dynamics in an Elongational Flow. *Science* **1997**, *276*, 2016−2021.
(100) de Gennes, P. G. Molecular Individualism. *Science* **1997**, *276*, 1999−2000.
(101) Jiang, Z.-C.; Xiao, Y.-Y.; Tong, X.; Zhao, Y. Selective Decrosslinking in Liquid Crystal Polymer Actuators for Optical Reconfiguration of Origami and Light-Fueled Locomotion. *Angew. Chem., Int. Ed.* **2019**, *58*, 5332−5337.
(102) Alexander-Katz, A. Toward Novel Polymer-Based Materials Inspired in Blood Clotting. *Macromolecules* **2014**, *47*, 1503−1513.

https://doi.org/10.1021/acs.jpcb.1c01819
J. Phys. Chem. B 2021, 125, 6373−6389